Electronic Supporting Information

a

David Villaman,[*a] Andrés Vega,[b] Lucía Santa María de la Parra,[c] Ignacio E. León,[c,d], Pedro Levín,[e] Patricia M. Toro*[f]

[a] Laboratorio de Química Inorgánica y Organometálica, Facultad de Cs. Química, Universidad de Concepción, Chile.
[b] Universidad Andrés Bello, Facultad de Ciencias Exactas, Departamento de Ciencias Químicas, Av. República 498, Santiago, Chile.
[c] CEQUINOR (UNLP, CCT-CONICET La Plata, Asociado a CIC), Departamento de Química, Facultad de Ciencias Exactas, Universidad Nacional de La Plata. Blvd. 120 N° 1465, La Plata 1900, Argentina;
[d] Cátedra de Fisiopatología, Departamento de Ciencias Biológicas, Facultad de Ciencias Exactas, Universidad Nacional de La Plata. 47 y 115, La Plata 1900, Argentina
[e] Departamento de Química de los Materiales, Facultad de Química y Biología, Universidad de Santiago de Chile, Av. Libertador Bernardo O'Higgins 3363, Estación Central, Santiago, Chile.
[f] Instituto de Ciencias Aplicadas, Facultad de Ingeniería, Universidad Autónoma de Chile, Talca, Chile.

*Corresponding author

E-mail addresses: dvillaman@udec.cl (D. Villaman), and patricia.toro@uautonoma.cl (P. M. Toro).

(66 pages)

Contents

1. Supplementary Tables

Table S1. Summary of experimental ultraviolet-visible spectroscopic data: position of the main bands detected [wavelengths λ_i (nm)] and logarithms of their molar extinction coefficients [log ε_i (ε_i in M^{-1} cm^{-1})] for compounds **Ni^{II}-L^1**, **Ni^{II}-L^2**, **Zn^{II}-L^1** and **Zn^{II}-L^2**.

Table S2. Crystallographic data for **H_2L^1** and **H_2L^2** .

Table S3. Crystallographic data for **Ni^{II}-L^1** and **Ni^{II}-L^2** .

Table S4. Bond lengths [Å] and angles [°] for **H_2L^1**.

Table S5. Bond lengths [Å] and angles [°] for **H_2L^2**.

Table S6. Intramolecular and intermolecular hydrogen bonds for **H_2L^1**.

Table S7. Intramolecular and intermolecular hydrogen bonds for **H_2L^2**.

Table S8. Bond lengths [Å] and angles [°] for **Ni^{II}-L^1**.

Table S9. Intermolecular hydrogen bonds for **Ni^{II}-L^1**.

Table S10. Bond lengths [Å] and angles [°] for **Ni^{II}-L^2**.

Table S11. Intermolecular hydrogen bonds for **Ni^{II}-L^2**.

2. Supplementary Figures

Figure S1. High resolution mass spectrum (HRMS) of compound **H_2L^1** asymmetric ligand. The peak at *m/z* 353.1497 corresponds to $[M + H]^+$.

Figure S2. High resolution mass spectrum (HRMS) of compound **H_2L^2** asymmetric ligand. The peak at *m/z* 405.1532 corresponds to $[M + Na]^+$.

Figure S3. High resolution mass spectrum (HRMS) of compound **Ni^{II}-L^1** asymmetric ligand. The peak at 409.0930 *m/z* corresponds to $[M + H]^+$.

Figure S4. High resolution mass spectrum (HRMS) of compound **Zn^{II}-L^1** asymmetric ligand. The peak at *m/z* 415.0630 corresponds to $[M]^+$.

Figure S5. High resolution mass spectrum (HRMS) of compound **Ni^{II}-L^2** asymmetric ligand. The peak at *m/z* 439.0803 corresponds to $[M + H]^+$.

Figure S6. High resolution mass spectrum (HRMS) of compound **Zn^{II}-L^2** asymmetric ligand. The peak at *m/z* 445.0740 corresponds to $[M]^+$.

Figure S7. FT-IR spectrum of 2-hidroxy-5-methoxybenzaldehyde in KBr disc.

Figure S8. FT-IR spectrum of salicylaldehyde in KBr disc.

Figure S9. FT-IR spectrum of *o*-phenylenediamine in KBr disc.

Figure S10. FT-IR spectrum of ethyl-2-(ethoxymethylene)acetoacetate in KBr disc.

Figure S11. FT-IR spectrum of compound $\mathbf{H_2L^1}$ in KBr disc.

Figure S12. FT-IR spectrum of compound $\mathbf{H_2L^1}$ in KBr disc.

Figure S13. FT-IR spectrum of compound $\mathbf{Ni^{II}\text{-}L^1}$ in KBr disc.

Figure S14. FT-IR spectrum of compound $\mathbf{Zn^{II}\text{-}L^1}$ in KBr disc.

Figure S15. FT-IR spectrum of compound $\mathbf{Ni^{II}\text{-}L^2}$ in KBr disc.

Figure S16. FT-IR spectrum of compound $\mathbf{Zn^{II}\text{-}L^2}$ in KBr disc.

Figure S17. (a) ^{1}H NMR spectrum (400 MHz) of compound $\mathbf{H_2L^1}$ in $CDCl_3$; (b) zoom-in of the aromatic region of the ^{1}H NMR spectrum of $\mathbf{H_2L^1}$.

Figure S18. (a) ^{1}H NMR spectrum (400 MHz) of compound $\mathbf{H_2L^2}$ in $CDCl_3$; (b) zoom-in of the aromatic region of the ^{1}H NMR spectrum of $\mathbf{H_2L^2}$.

Figure S19. (a) ^{1}H NMR spectrum (400 MHz) of compound $\mathbf{Ni^{II}\text{-}L^1}$ in $CDCl_3$; (b) zoom-in of the aromatic region of the ^{1}H NMR spectrum of $\mathbf{Ni^{II}\text{-}L^1}$.

Figure S20. (a) ^{1}H NMR spectrum (400 MHz) of compound $\mathbf{Zn^{II}\text{-}L^1}$ in $CDCl_3$; (b) zoom-in of the aromatic region of the ^{1}H NMR spectrum of $\mathbf{Zn^{II}\text{-}L^1}$.

Figure S21. (a) ^{1}H NMR spectrum (400 MHz) of compound $\mathbf{Ni^{II}\text{-}L^2}$ in $CDCl_3$; (b) zoom-in of the aromatic region of the ^{1}H NMR spectrum of $\mathbf{Ni^{II}\text{-}L^2}$.

Figure S22. (a) ^{1}H NMR spectrum (400 MHz) of compound $\mathbf{Zn^{II}\text{-}L^2}$ in $CDCl_3$; (b) zoom-in of the aromatic region of the ^{1}H NMR spectrum of $\mathbf{Zn^{II}\text{-}L^2}$.

Figure S23. ^{13}C NMR spectrum (400 MHz) of compound $\mathbf{H_2L^1}$ in $CDCl_3$.

Figure S24. ^{13}C NMR spectrum (400 MHz) of compound $\mathbf{H_2L^2}$ in $CDCl_3$.

Figure S25. ^{13}C NMR spectrum (400 MHz) of compound $\mathbf{Ni^{II}\text{-}L^1}$ in $CDCl_3$.

Figure S26. ^{13}C NMR spectrum (400 MHz) of compound $\mathbf{Zn^{II}\text{-}L^1}$ in $CDCl_3$.

Figure S27. ^{13}C NMR spectrum (400 MHz) of compound $\mathbf{Ni^{II}\text{-}L^2}$ in $CDCl_3$.

Figure S28. ^{13}C NMR spectrum (400 MHz) of compound $\mathbf{Zn^{II}\text{-}L^2}$ in $CDCl_3$.

Figure S29. [^{1}H-^{1}H] NOESY NMR spectrum (400 MHz) of compound $\mathbf{Ni^{II}\text{-}L^1}$ in $CDCl_3$. The NOESY spectrum of $\mathbf{Ni^{II}\text{-}L^1}$ shows the interaction between hydrogen at 8.19 ppm with two hydrogens atoms from aromatic region which is consistent with the assignation of the signal at 8.19 as imine group (CH=N).

Figure S30. ^{1}H NMR spectra of compound $\mathbf{H_2L^1}$ at different periods of storage (0, 4, 12, 24 and 48 h) in DMSO-d_6:D_2O solution (9:1) at 300 K.

Figure S31. ^{1}H NMR spectra of compound $\mathbf{H_2L^2}$ at different periods of storage (0, 4, 12, 24 and 48 h) in DMSO-d_6:D_2O solution (9:1) at 300 K.

Figure S32. ^{1}H NMR spectra of compound $\mathbf{Ni^{II}\text{-}L^1}$ at different periods of storage (0, 1, 4, 12, and 24 h) in DMSO-d_6:D_2O solution (9:1) at 300 K.

Figure S33. ^{1}H NMR spectra of compound $\mathbf{Zn^{II}\text{-}L^1}$ at different periods of storage (0, 4, 12, 24 and 48 h) in DMSO-d_6:D_2O solution (9:1) at 300 K.

Figure S34. ^{1}H NMR spectra of compound $\mathbf{Ni^{II}\text{-}L^2}$ at different periods of storage (0, 4, 12, 24 and 48 h) in DMSO-d_6:D_2O solution (9:1) at 300 K.

Figure S35. ^{1}H NMR spectra of compound $\mathbf{Zn^{II}\text{-}L^2}$ at different periods of storage (0, 1, 4, 12, and 24 h) in DMSO-d_6:D_2O solution (9:1) at 300 K.

Figure S36. The absorption spectrum of a freshly prepared solution of $\mathbf{Ni^{II}\text{-}L_1}$ in a DMSO:Buffer solution (60:40) and absorption spectral changes after several storage periods. **A)** Contains spectra registered every 3 h, up to 24 h, and in order to ease the visualization, **B)** contains a selection of the spectra obtained for t = 0, 12, and 24 h.

Figure S37. The absorption spectrum of a freshly prepared solution of $\mathbf{Ni^{II}\text{-}L_2}$ in a DMSO:Buffer solution (60:40) and absorption spectral changes after several storage periods. **A)** Contains spectra registered every 3 h, up to 24 h, and in order to ease the visualization, **B)** contains a selection of the spectra obtained for t = 0, 12, and 24 h.

Figure S38. The absorption spectrum of a freshly prepared solution of $\mathbf{Zn^{II}\text{-}L_1}$ in a DMSO:Buffer solution (60:40) and absorption spectral changes after several storage periods. **A)** Contains spectra registered every 3 h, up to 24 h, and in order to ease the visualization, **B)** contains a selection of the spectra obtained for t = 0, 12, and 24 h.

Figure S39. The absorption spectrum of a freshly prepared solution of $\mathbf{Zn^{II}\text{-}L_2}$ in a DMSO:Buffer solution (60:40) and absorption spectral changes after several storage periods. **A)** Contains spectra registered every 3 h, up to 24 h, and in order to ease the visualization, **B)** contains a selection of the spectra obtained for t = 0, 12, and 24 h.

Figure S40. Intermolecular hydrogen bonds C5-H5···O3 and C7-H7···O3 of compound $\mathbf{Ni^{II}\text{-}L^1}$.

Figure S41. Intermolecular bifurcated hydrogen bond C19-H19A···O1 and C19-H19A···O2 of compound **Ni^{II}-L^1**.

Figure S42. Intermolecular hydrogen bonds C21-H21C···O5 of compound **Ni^{II}-L^2**.

Figure S43. Intermolecular hydrogen bonds C19-H19B···O1 of compound **Ni^{II}-L^2**.

Figure S44. Cell viability assay on MG-63, HCT-116 and MDA-MB-231 cells after 24 of incubation with ligands (**H_2L^1 and H_2L^2**), Ni(II) complexes (**Ni^{II}-L^1 and Ni^{II}-L^2**) and Zn(II) complexes compound (**Zn^{II}-L^1 and Zn^{II}-L^2**). The results are expressed as the percentage of the basal level and represent the mean ± the standard error of the mean (SEM) (n = 18). Asterisk signficant difference in comparison with the basal level ($p < 0.01$).

Contents

1. Supplementary Tables

Table S1. Summary of experimental ultraviolet-visible spectroscopic data: position of the main bands detected [wavelengths λ_i (nm)] and logarithms of their molar extinction coefficients [log ε_i (ε_i in M^{-1} cm^{-1})] for compounds **Ni^{II}-L^1**, **Ni^{II}-L^2**, **Zn^{II}-L^1** and **Zn^{II}-L^2**.

	Compounds [a]			
	Ni^{II}-L^1	**Ni^{II}-L^2**	**Zn^{II}-L^1**	**Zn^{II}-L^2**
λ_1 (log ε_1)	353 (6.5)	357 (6.5)	353 (6.5)	358 (6.6)
λ_2 (log ε_2)	416 to 491 [b]	424 (6.6) 482 (6.7)	405 to 474 [b]	439 (6.6)

[a] Data obtained from the spectra recorded from fresh solutions of the compounds (t = 0 h).

[b] In this case the band is rather broad (see Figs. S36 and S37) and the position of the maximum cannot be determined accurately.

Table S2. Crystallographic data for $\mathbf{H_2L^1}$ and $\mathbf{H_2L^2}$.

	$\mathbf{H_2L^1}$	$\mathbf{H_2L^2}$
Empirical formula	$C_{20}H_{20}N_2O_4$	$C_{21}H_{22}N_2O_5$
Formula weight	352.38	382.40
T (K)	296.15	296.15
λ (Å)	0.71073	0.71073
Crystal system	monoclinic	orthorhombic
Space group	$P2_1/c$	*Pbca*
***a* (Å)**	11.9709(6)	22.8904(11)
***b* (Å)**	11.5289(5)	14.1561(6)
***c* (Å)**	14.3295(7)	24.2635(13)
α (°)	90	90
***b* (°)**	112.951(2)	90
γ (°)	90	90
V (Å^3)	1821.08(15)	7862.3(7)
Z	4	16
ρ_{calc} (g cm^{-3})	1.285	1.292
μ (mm^{-1})	0.090	0.093
F(000)	744.0	3232.0
Crystal size (mm^3)	0.25 × 0.24 × 0.049	0.24 × 0.21 × 0.19
2*θ* range (°)	From 4.692 to 64.212	From 4.576 to 56.676
Index ranges	$-17 \le h \le 15$	$-30 \le h \le 26$
	$-17 \le k \le 17$	$-18 \le k \le 15$
	$-20 \le l \le 21$	$-28 \le l \le 32$
Reflections collected	36211	51082
Independent reflections	6359 [R_{int} = 0.0494]	9795 [R_{int} = 0.0565]
Data/restraints/paramet	6359/238	9795/7/524
Goodness-of-fit on F^2	1.031	1.002
Final *R* indices [*I* > 2s(*I*)]	R_1 = 0.0546, wR_2 = 0.1596	R_1 = 0.0579, wR_2 = 0.1485
***R* indices (all data)**	R_1 = 0.0855, wR_2 = 0.1849	R_1 = 0.1167, wR_2 = 0.1876

Table S3. Crystallographic data for Ni^{II}-L^1 and Ni^{II}-L^2.

	Ni^{II}-L^1	Ni^{II}-L^2
Empirical formula	$C_{20}H_{18}N_2NiO_4$	$C_{21}H_{20}N_2NiO_5$
Formula weight	409.07	439.10
T (K)	296.15	296.15
λ (Å)	0.71073	0.71073
Crystal system	monoclinic	Triclinic
Space group	$P2_1/c$	P-1
***a* (Å)**	11.2066(7)	8.142(5)
***b* (Å)**	11.7649(9)	10.284(5)
***c* (Å)**	13.5458(10)	11.733(6)
α (°)	90	90.098(16)
***b* (°)**	102.150(3)	93.951(16)
γ (°)	90	100.460(12)
V (Å^3)	1745.9(2)	963.8(9)
Z	4	2
ρ_{calc} (g cm^{-3})	1.556	1.513
μ (mm^{-1})	1.141	1.043
F(000)	848.0	456.0
Crystal size (mm^3)	0.2 × 0.097 × 0.049	0.3 × 0.16 × 0.054
2θ range (°)	From 4.632 to 66.492	From 5.362 to 61.902
Index ranges	$-17 \le h \le 16$	$-11 \le h \le 11$
	$-18 \le k \le 18$	$-14 \le k \le 14$
	$-20 \le l \le 20$	$-16 \le l \le 16$
Reflections collected	36870	33528
Independent reflections	6680 [R_{int} = 0.0642]	6042 [R_{int} = 0.0551]
Data/parameters	6680/246	6042/265
Goodness-of-fit on F^2	1.014	1.090
Final *R* indices [$I > 2\sigma(I)$]	R_1 = 0.0439, wR_2 = 0.1017	R_1 = 0.0436, *w*R_2 = 0.1134
***R* indices (all data)**	R_1 = 0.0727, wR_2 = 0.1156	R_1 = 0.0689, *w*R_2 = 0.1347

Table S4. Bond lengths [Å] and angles [°] for H_2L^1.

Atoms	Length/Å	Atoms	Length/Å
O1-C1	1.343(2)	**C5-C6**	1.399(2)
O2-C16	1.2422(17)	**C6-C7**	1.4490(19)
O3-C18	1.2052(16)	**C8-C9**	1.3912(17)
O4-C18	1.3417(17)	**C8-C13**	1.4009(18)
O4-C19	1.4358(19)	**C9-C10**	1.378(2)
N1-C7	1.2839(18)	**C10-C11**	1.378(2)
N1-C8	1.4148(16)	**C11-C12**	1.383(2)
N2-C13	1.4015(15)	**C12-C13**	1.3906(18)
N2-C14	1.3234(17)	**C14-C15**	1.3839(17)
C1-C2	1.390(2)	**C15-C16**	1.4529(19)
C1-C6	1.402(2)	**C15-C18**	1.4685(18)
C2-C3	1.377(3)	**C16-C17**	1.492(2)
C3-C4	1.373(3)	**C19-C20**	1.481(3)
C4-C5	1.375(2)		
Atoms	**Angles/°**	**Atoms**	**Angles/°**
C18-O4-C19	117.01(12)	**C9-C10-C11**	119.72(13)
C7-N1-C8	118.30(11)	**C10-C11-C12**	120.53(13)
C14-N2-C13	127.34(12)	**C11-C12-C13**	120.04(14)
O1-C1-C2	118.22(15)	**C8-C13-N2**	117.55(11)
O1-C1-C6	122.42(14)	**C12-C13-N2**	122.72(12)
C2-C1-C6	119.36(16)	**C12-C13-C8**	119.73(11)
C3-C2-C1	120.41(18)	**N2-C14-C15**	124.86(13)
C4-C3-C2	120.75(17)	**C14-C15-C16**	120.31(12)
C3-C4-C5	119.69(18)	**C14-C15-C18**	117.87(12)
C4-C5-C6	120.94(17)	**C16-C15-C18**	121.82(11)
C1-C6-C7	122.57(14)	**O2-C16-C15**	120.34(12)
C5-C6-C1	118.82(14)	**O2-C16-C17**	117.85(13)
C5-C6-C7	118.60(13)	**C15-C16-C17**	121.78(13)
N1-C7-C6	123.67(12)	**O3-C18-O4**	121.57(13)
C9-C8-N1	122.83(12)	**O3-C18-C15**	126.21(13)
C9-C8-C13	118.93(12)	**O4-C18-C15**	112.20(11)
C13-C8-N1	118.20(11)	**O4-C19-C20**	108.68(16)
C10-C9-C8	121.02(14)		

Table S5. Bond lengths [Å] and angles [°] for H_2L^2.

Atoms	Length/Å	Atoms	Length/Å
O1A-C1A	1.359(3)	**O1B-C1B**	1.356(3)
O2A-C16A	1.241(3)	**O2B-C16B**	1.241(3)
O3A-C18A	1.204(3)	**O3B-C18B**	1.196(3)
O4A-C18A	1.319(4)	**O4B-C18B**	1.329(3)
O4A-C19A	1.462(3)	**O4B-C19B**	1.451(3)
O5A-C4A	1.370(3)	**O5B-C4B**	1.376(3)
O5A-C4A	1.413(4)	**O5B-C21B**	1.403(4)
N1A-C7A	1.284(3)	**N1B-C7B**	1.287(3)
N1A-C8A	1.420(3)	**N1B-C8B**	1.419(3)
N2A-C13A	1.406(2)	**N2B-C13B**	1.403(3)
N2A-C14A	1.327(2)	**N2B-C14B**	1.328(2)
C1A-C2A	1.384(3)	**C1B-C2B**	1.389(4)
C1A-C6A	1.391(3)	**C1B-C6B**	1.386(3)
C2A-C3A	1.360(4)	**C2B-C3B**	1.365(4)
C3A-C4A	1.381(3)	**C3B-C4B**	1.369(4)
C4A-C5A	1.367(3)	**C4B-C5B**	1.365(3)
C5A-C6A	1.408(3)	**C5B-C6B**	1.404(3)
C6A-C7A	1.440(3)	**C6B-C7B**	1.445(3)
C8A-C9A	1.389(3)	**C8B-C9B**	1.385(3)
C8A-C13A	1.395(3)	**C8B-C13B**	1.397(3)
C9A-C10A	1.377(3)	**C9B-C10B**	1.382(3)
C10A-C11A	1.371(3)	**C10B-C11B**	1.371(3)
C11A-C12A	1.369(3)	**C11B-C12B**	1.368(3)
C12A-C13A	1.389(3)	**C12B-C13B**	1.387(3)
C14A-C15A	1.380(3)	**C14B-C15B**	1.376(3)
C15A-C16A	1.432(4)	**C15B-C16B**	1.440(4)
C15A-C18A	1.466(3)	**C15B-C18B**	1.464(3)
C16A-C19A	1.506(3)	**C16B-C17B**	1.510(3)
C19A-C20	1.427(13)	**C19B-C20B**	1.468(5)
C19A-C20A	1.434(12)		
Atoms	**Angle/°**	**Atoms**	**Angle/°**
C18A-O4A-C19A	115.5(3)	**C19B-O4B-C20B**	116.4(2)
C4A-O5A-C21A	117.3(2)	**C4B-O5B-C5B**	117.0(3)

C7A-N1A-C8A	118.18(17)	**C7B-N1B-C8B**	118.62(18)
C14A-N2A-C13A	126.75(19)	**C14B-N2B-C13B**	125.9(2)
O1A-C1A-C2A	118.6(2)	**O1B-C1B-C2B**	118.4(2)
O1A-C1A-C6A	122.0(2)	**O1B-C1B-C6B**	122.4(2)
C2A-C1A-C6A	119.4(2)	**C6B-C1B-C2B**	119.1(3)
C3A-C2A-C1A	120.6(2)	**C3B-C2B-C1B**	120.2(3)
C2A-C3A-C4A	121.0(2)	**C2B-C3B-C4B**	121.4(3)
O5A-C4A-C3A	115.7(2)	**C3B-C4B-O5B**	115.6(3)
C5A-C4A-O5A	124.8(2)	**C5B-C4B-O5B**	125.2(3)
C5A-C4A-C3A	119.5(2)	**C5B-C4B-C3B**	119.2(3)
C4A-C5A-C6A	120.4(2)	**C4B-C5B-C6B**	120.8(2)
C1A-C6A-C5A	119.1(2)	**C1B-C6B-C5B**	119.2(2)
C1A-C6A-C7A	122.6(2)	**C1B-C6B-C7B**	122.3(2)
C5A-C6A-C7A	118.25(19)	**C5B-C6B-C7B**	118.5(2)
N1A-C7A-C6A	123.4(2)	**N1B-C7B-C6B**	123.6(2)
C9A-C8A-N1A	122.60(18)	**C9B-C8B-N1B**	122.20(18)
C9A-C8A-C13A	119.43(19)	**C9B-C8B-C13B**	119.1(2)
C13A-C8A-N1A	117.93(17)	**C13B-C8B-N1B**	118.61(18)
C10A-C9A-C8A	120.4(2)	**C10B-C9B-C9B**	120.7(2)
C11A-C10A-C9A	119.8(2)	**C11B-C10B-C9B**	119.7(2)
C12A-C11A-C10A	120.8(2)	**C12B-C11B-C10B**	120.5(2)
C11A-C12A-C13A	120.3(2)	**C11B-C12B-C13B**	120.6(2)
C8A-C13A-N2A	118.17(18)	**C8B-C13B-N2B**	118.31(19)
C12A-C13A-N2A	122.58(18)	**C12B-C13B-N2B**	122.34(18)
C12A-C13A-C8A	119.24(18)	**C12B-C13B-C8B**	119.33(19)
N2A-C14A-C15A	125.6(2)	**N2B-C14B-C15B**	126.3(2)
C14A-C15A-C16A	121.1(2)	**C14B-C15B-C16B**	120.8(2)
C14A-C15A-C18A	117.4(3)	**C14B-C15B-C18B**	117.4(2)
C16A-C17A-C18A	121.5(2)	**C16B-C15B-C18B**	121.9(2)
O2A-C16A-C15A	120.3(2)	**O2B-C16B-C15B**	120.1(2)
O2A-C16A-C17A	117.3(3)	**O2B-C16B-C17B**	118.0(3)
C15A-C16A-C17A	122.4(3)	**C15B-C16B-C17B**	121.9(3)
O3A-C18A-O4A	121.3(3)	**O3B-C18B-O4B**	121.9(3)
O3A-C18A-C15A	125.9(3)	**O3B-C18B-C15B**	126.2(3)
O4A-C18A-C15A	112.8(2)	**O4B-C18B-C15B**	112.0(2)
C20-C19A-O4A	106.1(10)	**O4B-C19B-C20B**	106.7(3)
C20A-C19A-O4A	106.9(8)		

Table S6. Intramolecular and intermolecular hydrogen bonds for H_2L^1.

D-H···A	d(D-H)/Å	d(H-A)/Å	d(D-A)/Å	D-H-A/°
O1-H1···N1	0.82	1.98	2.7007(15)	146.1
N2-H2···O2	0.86	1.93	2.5951(14)	133.7
C19-H19A···O2^{i}	0.97	2.53	3.461(3)	161.0
C5-H5···O3^{ii}	0.93	2.76	3.523(2)	139.6
C7-H7···O3^{ii}	0.93	2.82	3.5947(17)	142.0
C20-H20A···O1^{iii}	0.96	2.85	3.569(3)	132.5
^{i} 1-x, -1/2+y, 3/2-z, ^{ii} +x, 1+y, +z, ^{iii} 1-x, 1-y, 1-z				

Table S7. Intramolecular and intermolecular hydrogen bonds for H_2L^2.

D-H···A	d(D-H)/Å	d(H-A)/Å	d(D-A)/Å	D-H-A/°
O1A-H1A···N1A	0.82	1.97	2.678(2)	143.3
N2A-H2A···O2A	0.86	1.96	2.613(2)	131.8
O1B-H1B···N1B	0.82	1.97	2.676(3)	144.2
N2B-H2B···O2B	0.86	1.97	2.617(3)	130.7
C9A-H9A···O3A^{iv}	0.93	2.39	3.283(3)	160.7
C9A-H9A···O3A^{v}	0.93	2.31	3.146(3)	149.3
C5A-H5A···O2B	0.93	2.44	3.338(3)	162.1
C5B-H5B···O2A	0.93	2.46	3.348(3)	161.0
^{iv} -1/2+y, +y, ½-z; ^{v} 1/2+x, +y,1/2-z				

Table S8. Bond lengths [Å] and angles [°] for $\mathbf{Ni^{II}}$-$\mathbf{L^1}$.

Atoms	Length/Å	Atoms	Length/Å
Ni1-O1	1.8479(13)	**C3-C4**	1.390(3)
Ni1-O2	1.8556(12)	**C4-C5**	1.366(3)
Ni1-N1	1.8526(13)	**C5-C6**	1.412(3)
Ni1-N2	1.8461(15)	**C6-C7**	1.409(2)
O1-C1	1.300(2)	**C8-C9**	1.394(2)
O2-C16	1.268(2)	**C8-C13**	1.396(2)
O3-C18	1.213(2)	**C9-C10**	1.372(3)
O4-C18	1.341(3)	**C10-C11**	1.387(3)
O4-C19	1.452(2)	**C11-C12**	1.383(3)
N1-C7	1.305(2)	**C12-C13**	1.391(3)
N1-C8	1.416(2)	**C14-C15**	1.408(2)
N2-C13	1.419(2)	**C15-C16**	1.414(3)
N2-C14	1.310(2)	**C15-C18**	1.477(2)
C1-C2	1.417(3)	**C16-C17**	1.506(3)
C1-C6	1.418(2)	**C19-C20**	1.492(4)
C2-C3	1.369(3)		
Atoms	**Angle/°**	**Atoms**	**Angle/°**
O1-Ni1-O2	85.54(6)	**C7-C6-C5**	117.51(17)
O1-Ni1-N1	95.41(6)	**N1-C7-C6**	125.15(16)
N1-Ni1-O2	178.97(6)	**C9-C8-N1**	125.94(16)
N2-Ni1-O1	178.44(6)	**C9-C8-C13**	120.61(17)
N2-Ni1-O2	92.98(6)	**C13-C8-N1**	113.45(15)
N2-Ni1-N1	86.07(6)	**C10-C9-C8**	118.94(18)
C1-O1-Ni1	127.02(12)	**C9-C10-C11**	120.92(19)
C16-O2-Ni1	130.58(12)	**C12-C11-C10**	120.52(19)
C18-O4-C19	117.95(16)	**C11-C12-C13**	119.35(18)
C7-N1-Ni1	125.85(13)	**C8-C13-N2**	113.43(16)
C7-N1-C8	120.65(14)	**C12-C13-N2**	126.90(17)
C8-N1-Ni1	113.46(11)	**C12-C13-C8**	119.66(16)
C13-N2-Ni1	113.54(11)	**N2-C14-C15**	126.65(17)
C14-N2-Ni1	125.99(13)	**C14-C15-C16**	120.53(16)
C14-N2-C13	120.46(16)	**C14-C15-C18**	117.01(17)
O1-C1-C2	119.30(17)	**C16-C15-C18**	122.43(16)

O1-C1-C6	124.04(17)	**O2-C16-C15**	123.15(16)
C2-C1-C6	116.66(18)	**O2-C16-C17**	114.18(17)
C3-C2-C1	121.7(2)	**C15-C16-C17**	122.66(16)
C2-C3-C4	121.0(2)	**O3-C18-O4**	121.82(18)
C5-C4-C3	119.3(2)	**O3-C18-C15**	127.00(19)
C4-C5-C6	121.1(2)	**O4-C18-C15**	111.17(16)
C5-C6-C1	120.20(18)	**O4-C19-C20**	107.33(19)
C7-C6-C1	122.29(16)		

Table S9. Intermolecular hydrogen bonds for **Ni^{II}-L^1**.

D-H···A	d(D-H)/Å	d(H-A)/Å	d(D-A)/Å	D-H-A/°
C5-H5···O3^{vi}	0.93	2.90	3.762(3)	155.1
C7-H7···O3^{vi}	0.93	2.83	3.717(2)	161.0
C9-H9···O3^{vi}	0.93	3.02	3.946(3)	176.0
C19-H19B···O1^{vii}	0.97	2.76	3.523(3)	136.5
C19-H19A···O1^{vii}	0.97	2.92	3.799(3)	151.7
C19-H19A···O2^{viii}	0.97	2.78	3.398(3)	122.2
^{vi} +x, -1+y, +z; ^{vii} 1-x,1/2+y,3/2-z; ^{viii} 1-x,1-y,1-z				

Table S10. Bond lengths [Å] and angles [°] for Ni^{II}-L^2.

Atoms	Length/Å	Atoms	Length/Å
Ni1-O1	1.8357(18)	**C2-C3**	1.364(4)
Ni1-O2	1.8594(18)	**C3-C4**	1.411(4)
Ni1-N1	1.8631(19)	**C4-C5**	1.379(3)
Ni1-N2	1.854(2)	**C5-C6**	1.429(3)
O1-C1	1.304(3)	**C6-C7**	1.424(3)
O2-C16	1.271(3)	**C8-C9**	1.397(3)
O3-C17	1.214(3)	**C8-C13**	1.397(3)
O4-C18	1.349(4)	**C9-C10**	1.397(3)
O4-C19	1.460(3)	**C10-C11**	1.382(4)
O5-C4	1.376(3)	**C11-C12**	1.390(4)
O5-C21	1.418(4)	**C12-C13**	1.401(3)
N1-C7	1.298(3)	**C14-C15**	1.423(3)
N1-C8	1.437(3)	**C15-C16**	1.412(4)
N2-C13	1.420(3)	**C15-C18**	1.477(3)
N2-C14	1.313(3)	**C16-C17**	1.522(3)
C1-C6	1.429(3)	**C19-C20**	1.472(3)
Atoms	**Angles/°**	**Atoms**	**Angles/°**
O1-Ni1-O2	83.93(8)	**C1-C6-C5**	119.9(2)
O1-Ni1-N1	96.02(8)	**C7-C6-C1**	121.7(2)
O1-Ni1-N2	177.80(8)	**C7-C6-C5**	118.4(2)
O2-Ni1-N1	178.76(7)	**N1-C7-C6**	125.3(2)
N2-Ni1-O2	94.02(8)	**C9-C8-N1**	126.5(2)
N2-Ni1-N1	86.05(8)	**C13-C8-N1**	112.99(19)
C1-O1-Ni1	126.87(15)	**C13-C8-C9**	120.5(2)
C16-O2-Ni1	129.85(16)	**C8-C9-C10**	119.1(2)
C18-O4-C19	116.3(2)	**C11-C10-C9**	120.6(2)
C4-O5-C21	117.4(2)	**C10-C11-C12**	120.6(2)
C7-N1-Ni1	125.67(15)	**C11-C12-C13**	119.6(2)
C7-N1-C8	121.19(19)	**C8-C13-N2**	114.04(19)
C8-N1-Ni1	113.11(14)	**C8-C13-C12**	119.6(2)
C13-N2-Ni1	113.56(15)	**C12-C13-N2**	126.3(2)
C14-N2-Ni1	124.95(16)	**N2-C14-C15**	126.7(2)
C14-N2-C13	121.5(2)	**C14-C15-C18**	117.9(2)
O1-C1-C2	117.7(2)	**C16-C15-C14**	120.9(2)

O1-C1-C6	124.4(2)	**C16-C15-C18**	121.2(2)
C6-C1-C2	117.8(2)	**O2-C16-C15**	123.3(2)
C3-C2-C1	121.0(2)	**O2-C16-C17**	112.9(2)
C2-C3-C4	121.2(2)	**C15-C16-C17**	123.8(2)
O5-C4-C3	114.8(2)	**O3-C18-O4**	122.1(3)
O5-C4-C5	125.2(2)	**O3-C18-C15**	126.2(3)
C5-C4-C3	120.0(2)	**O4-C18-C15**	111.7(2)
C4-C5-C6	120.0(2)	**O4-C19-C20**	108.4(3)

Table S11. Intermolecular hydrogen bonds for **Ni^{II}-L^2**.

D-H···A	d(D-H)/Å	d(H-A)/Å	d(D-A)/Å	D-H-A/°
C21-H21C···O5^{ix}	0.96	2.60	3.309(4)	131.3
C19-H19B···O1^{x}	0.97	2.71	3.541(4)	143.8
^{ix} 2-x, 2-y, 2-z ^{x} 1-x, -y,1-z;				

2. Supplementary Figures

Figure S1. High resolution mass spectrum (HRMS) of compound $\mathbf{H_2L^1}$ asymmetric ligand. The peak at *m/z* 353.1497 corresponds to $[M + H]^+$.

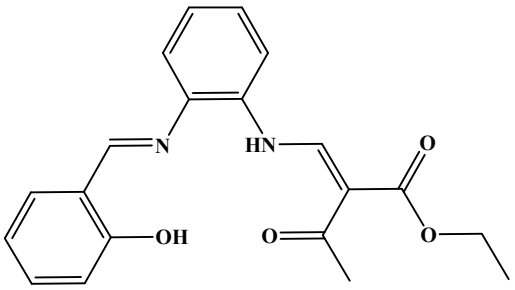

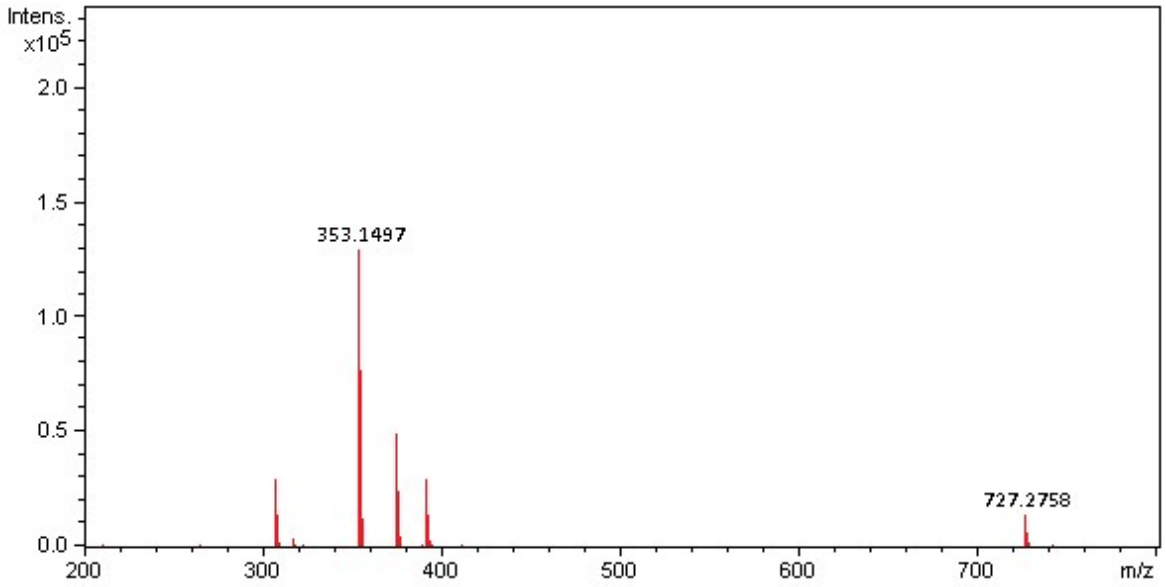

Figure S2. High resolution mass spectrum (HRMS) of compound $\mathbf{H_2L^2}$ asymmetric ligand. The peak at *m/z* 405.1532 corresponds to $[M + Na]^+$.

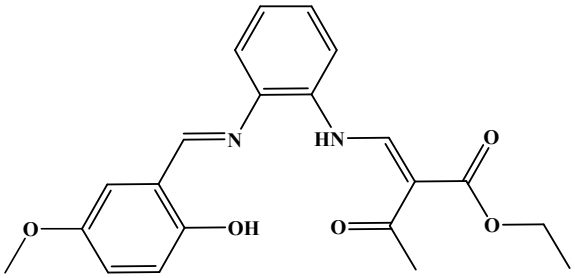

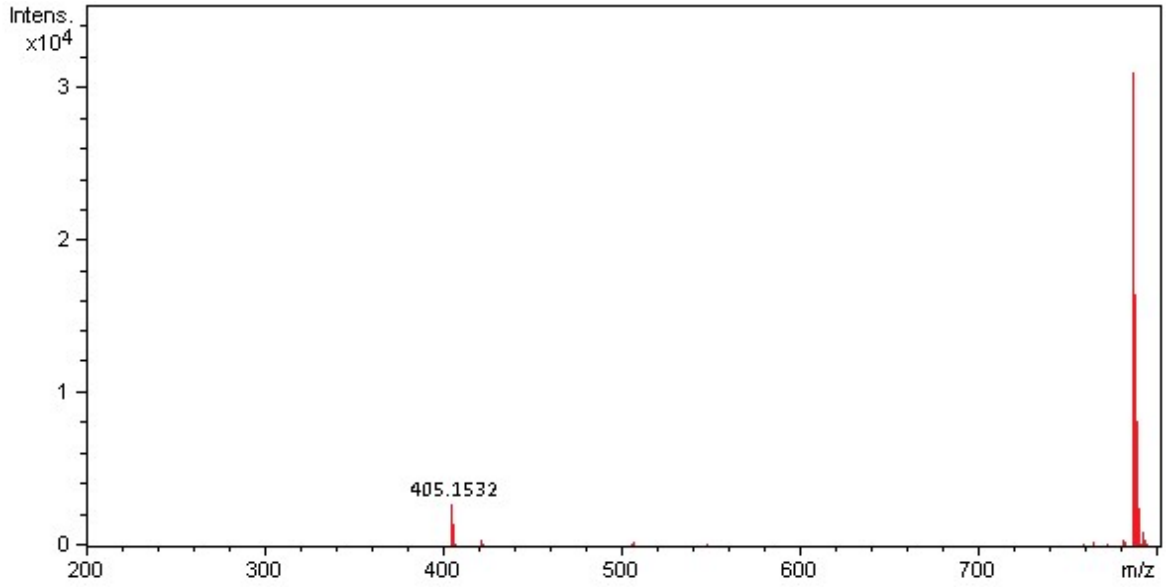

Figure S3. High resolution mass spectrum (HRMS) of compound $\mathbf{Ni^{II}\text{-}L^{1}}$ asymmetric ligand. The peak at *m/z* 409.0930 corresponds to $[M + H]^+$.

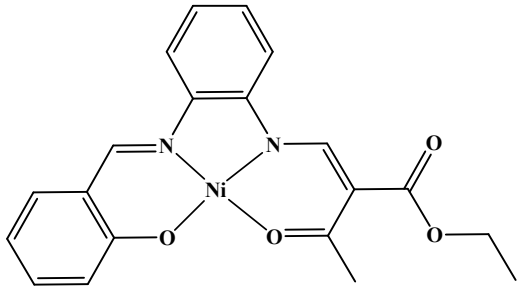

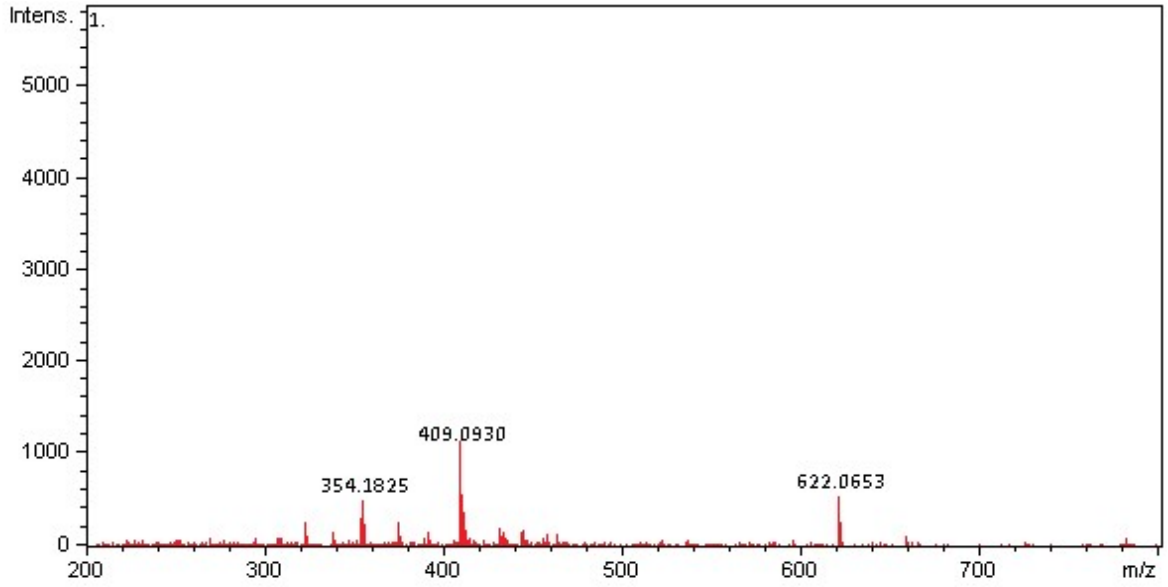

Figure S4. High resolution mass spectrum (HRMS) of compound **Zn^{II}-L^1** asymmetric ligand. The peak at *m/z* 415.0630 corresponds to $[M\ ]^+$.

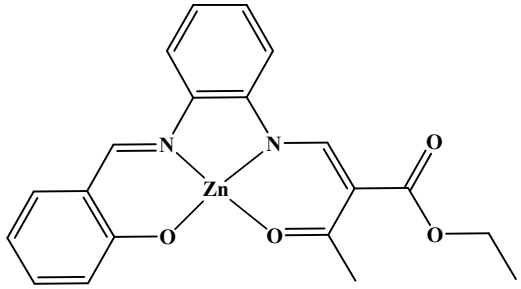

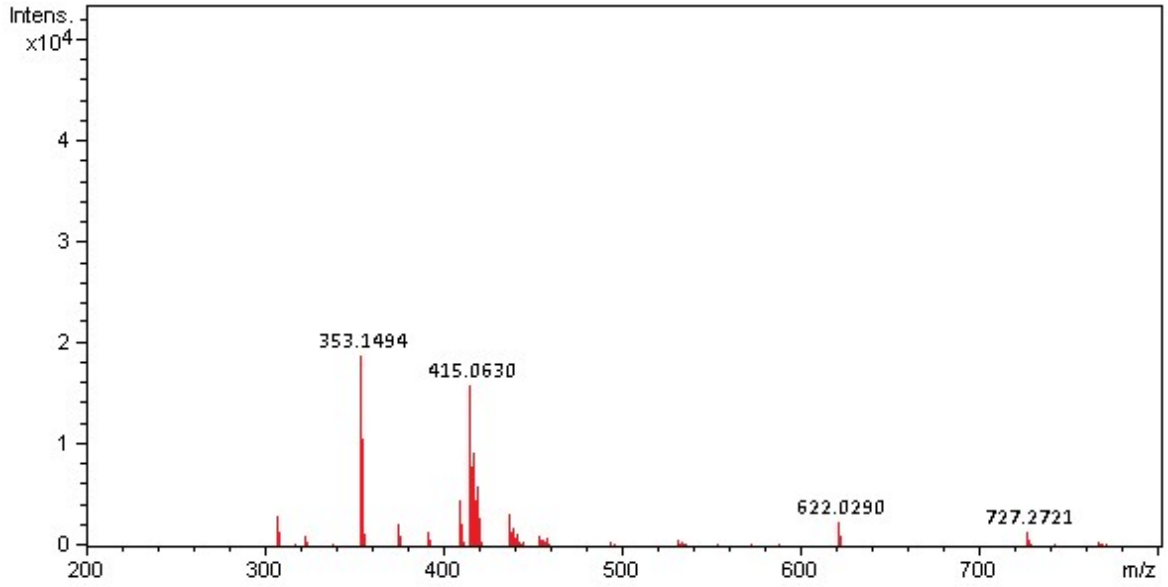

Figure S5. High resolution mass spectrum (HRMS) of compound **Ni^{II}-L^2** asymmetric ligand. The peak at *m/z* 439.0803 corresponds to $[M + H]^+$.

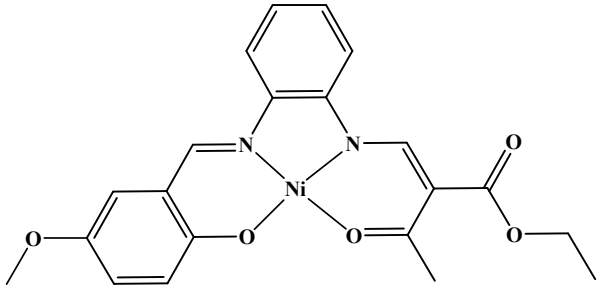

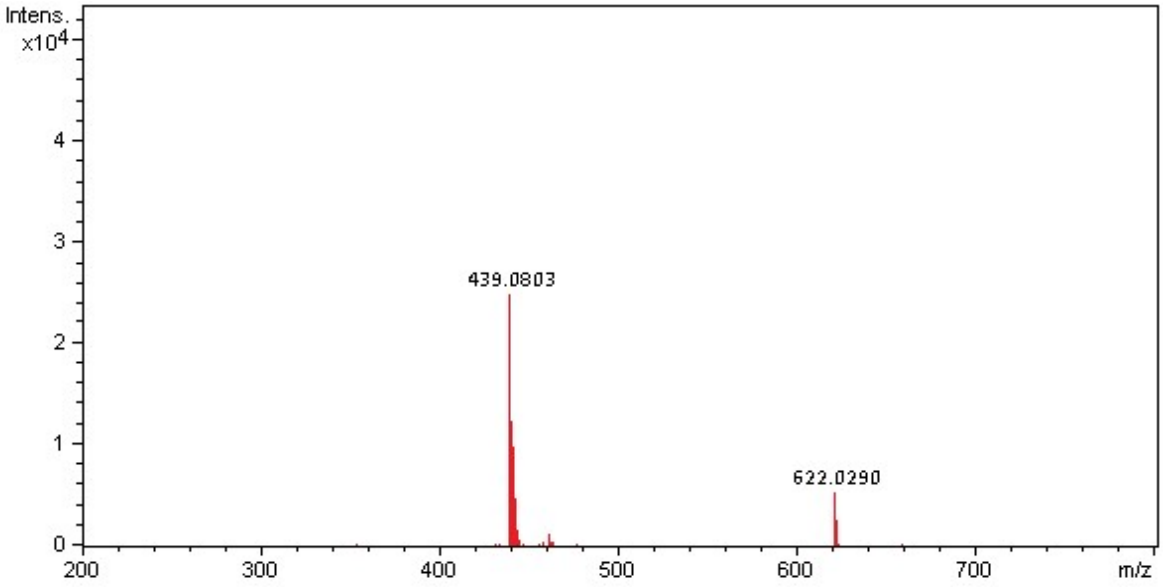

Figure S6. High resolution mass spectrum (HRMS) of compound **Zn^{II}-L^2** asymmetric ligand. The peak at *m/z* 445.0740 corresponds to $[M]^+$.

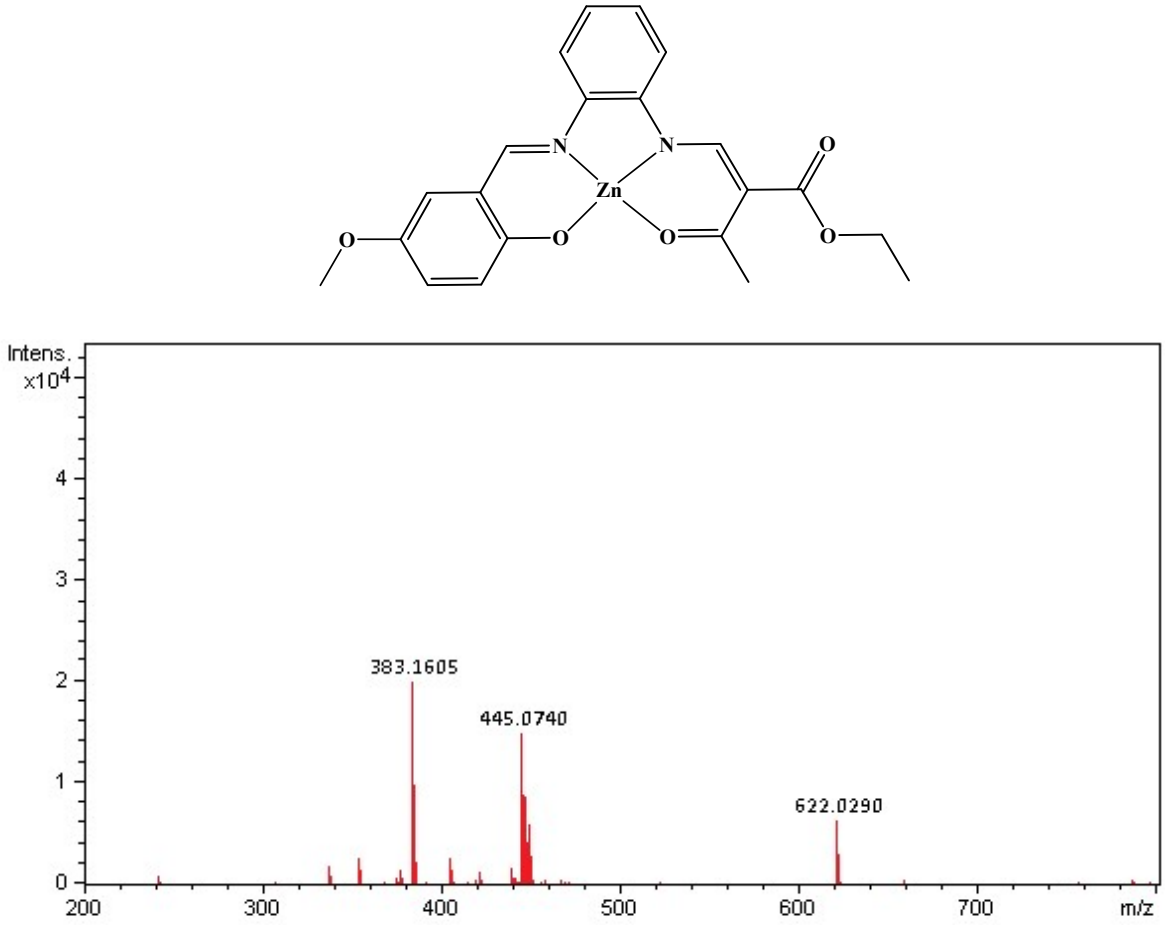

Figure S7. FT-IR spectrum of 2-hidroxy-5-methoxybenzaldehyde in KBr disc.

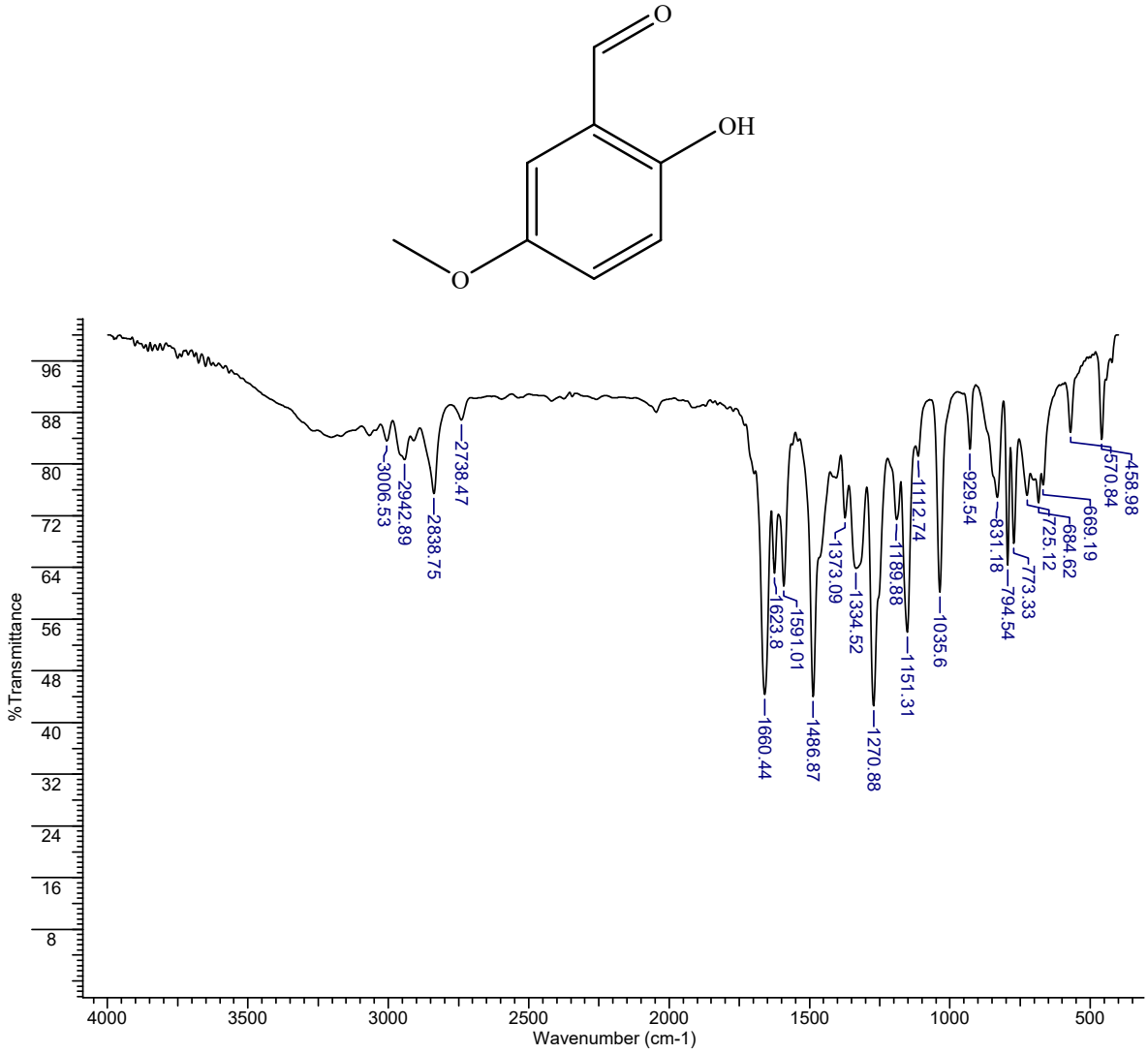

Figure S8. FT-IR spectrum of salicylaldehyde in KBr disc.

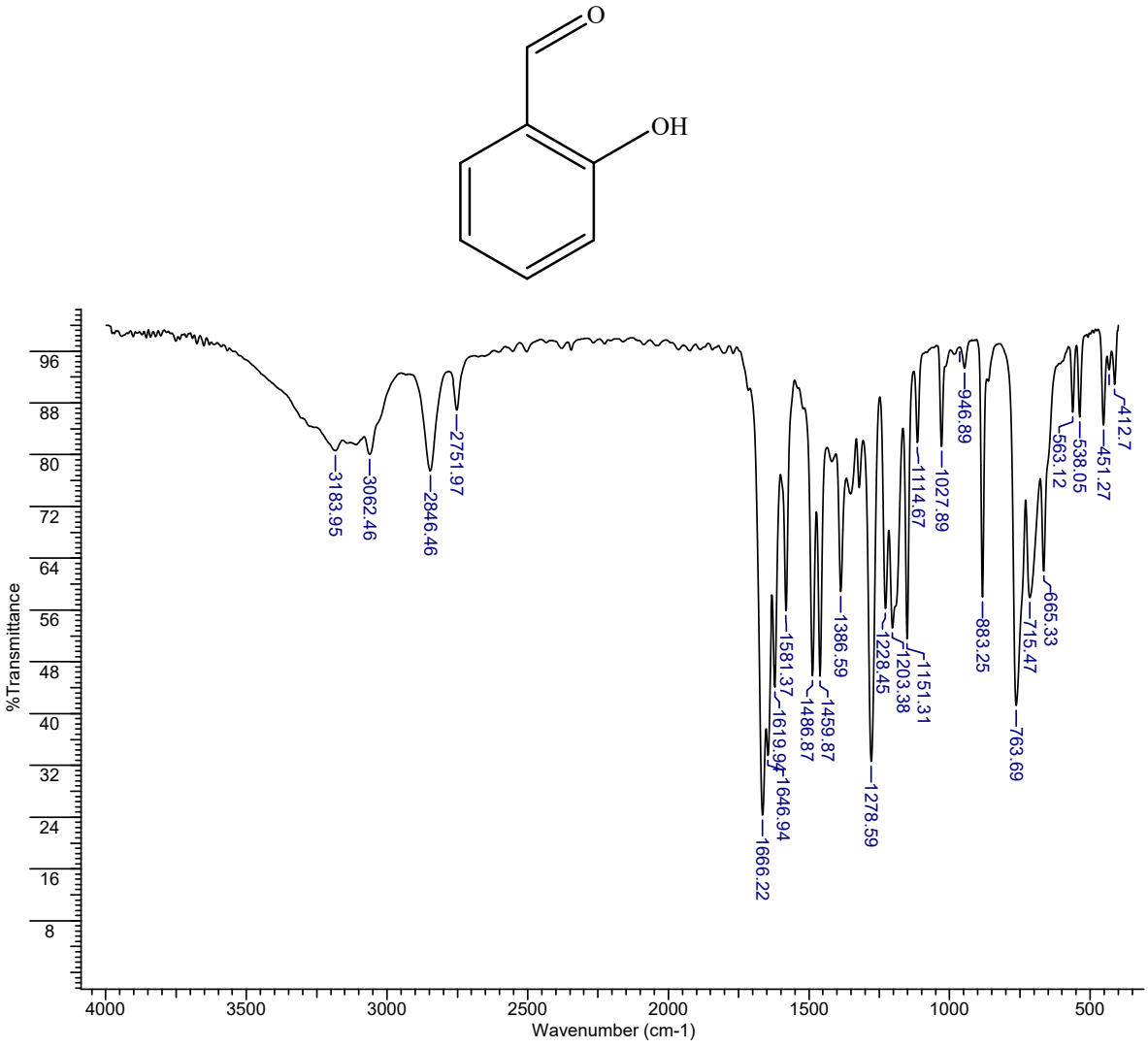

Figure S9. FT-IR spectrum of *o*-phenylenediamine in KBr disc.

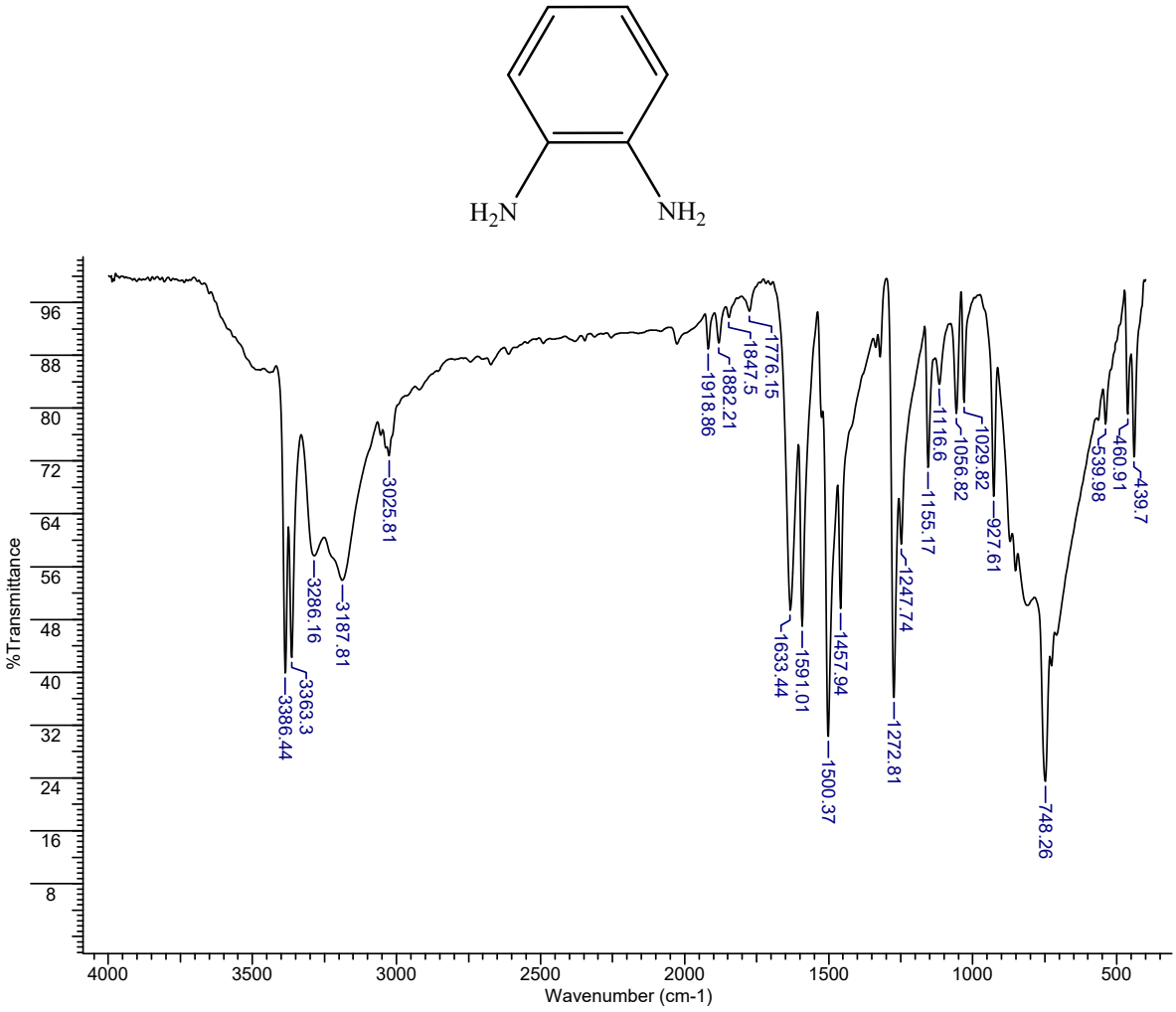

Figure S10. FT-IR spectrum of ethyl-2-(ethoxymethylene)acetoacetate in KBr disc.

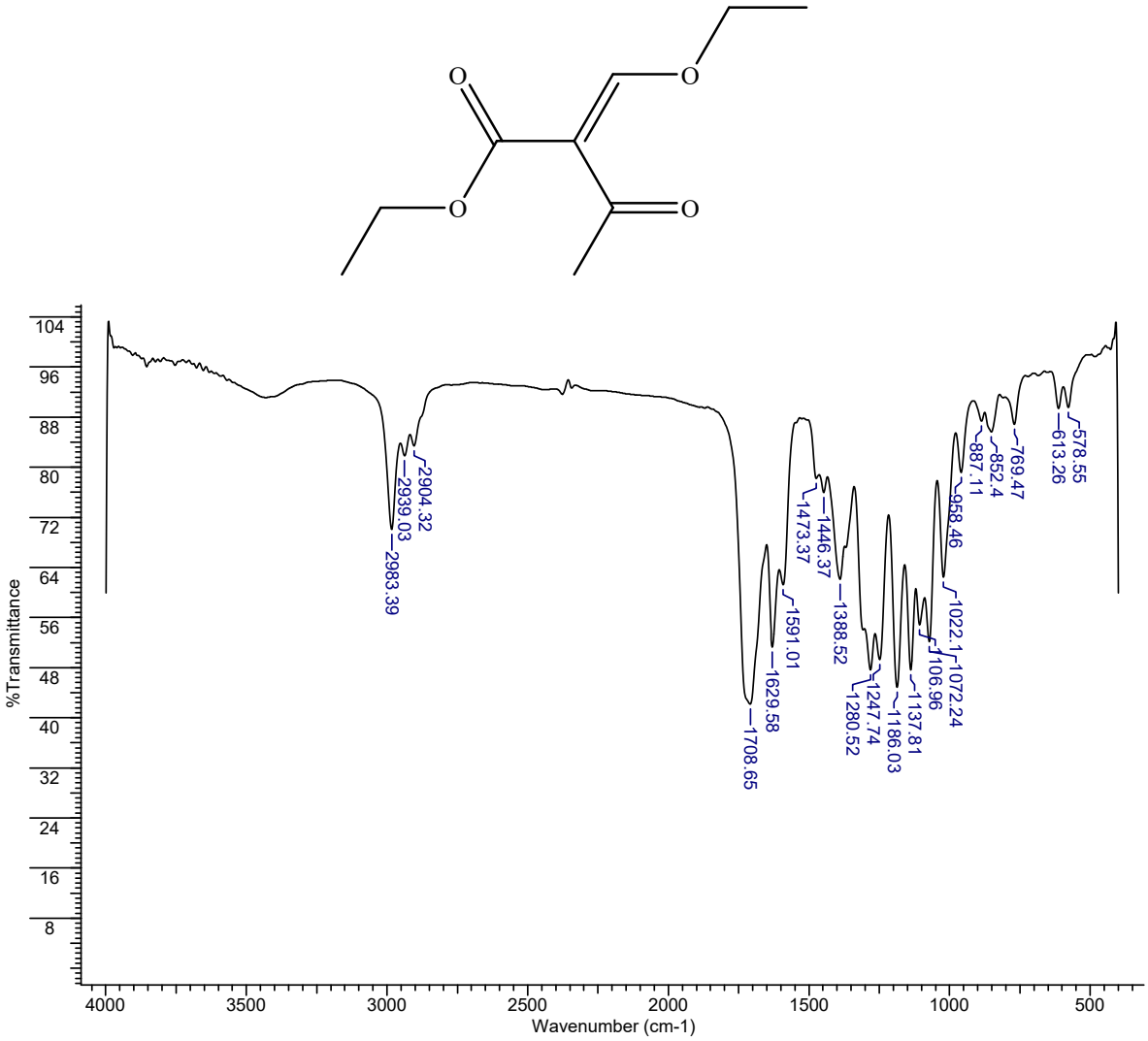

Figure S11. FT-IR spectrum of compound $\mathbf{H_2L^1}$ in KBr disc.

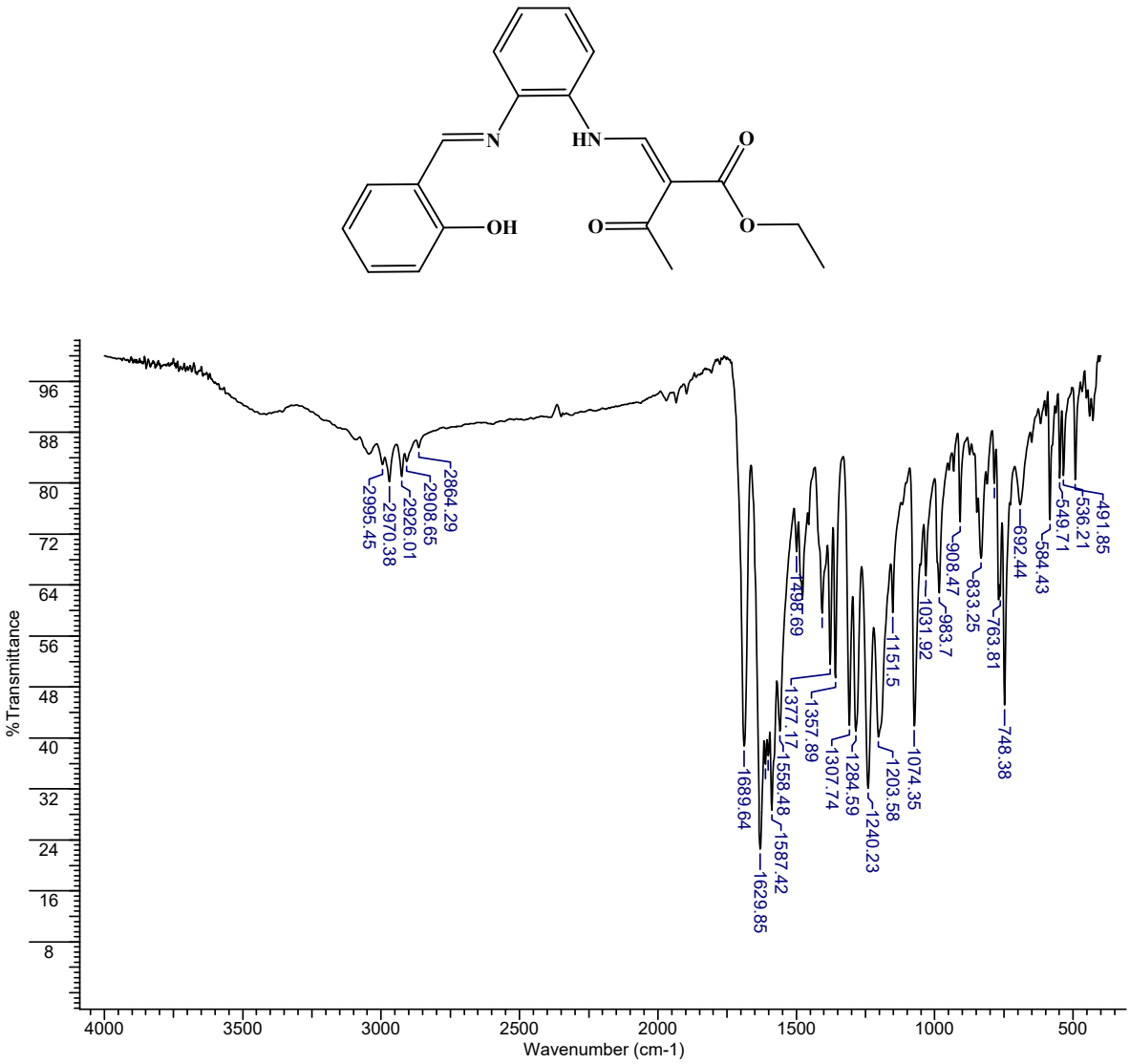

Figure S12. FT-IR spectrum of compound $\mathbf{H_2L^2}$ in KBr disc.

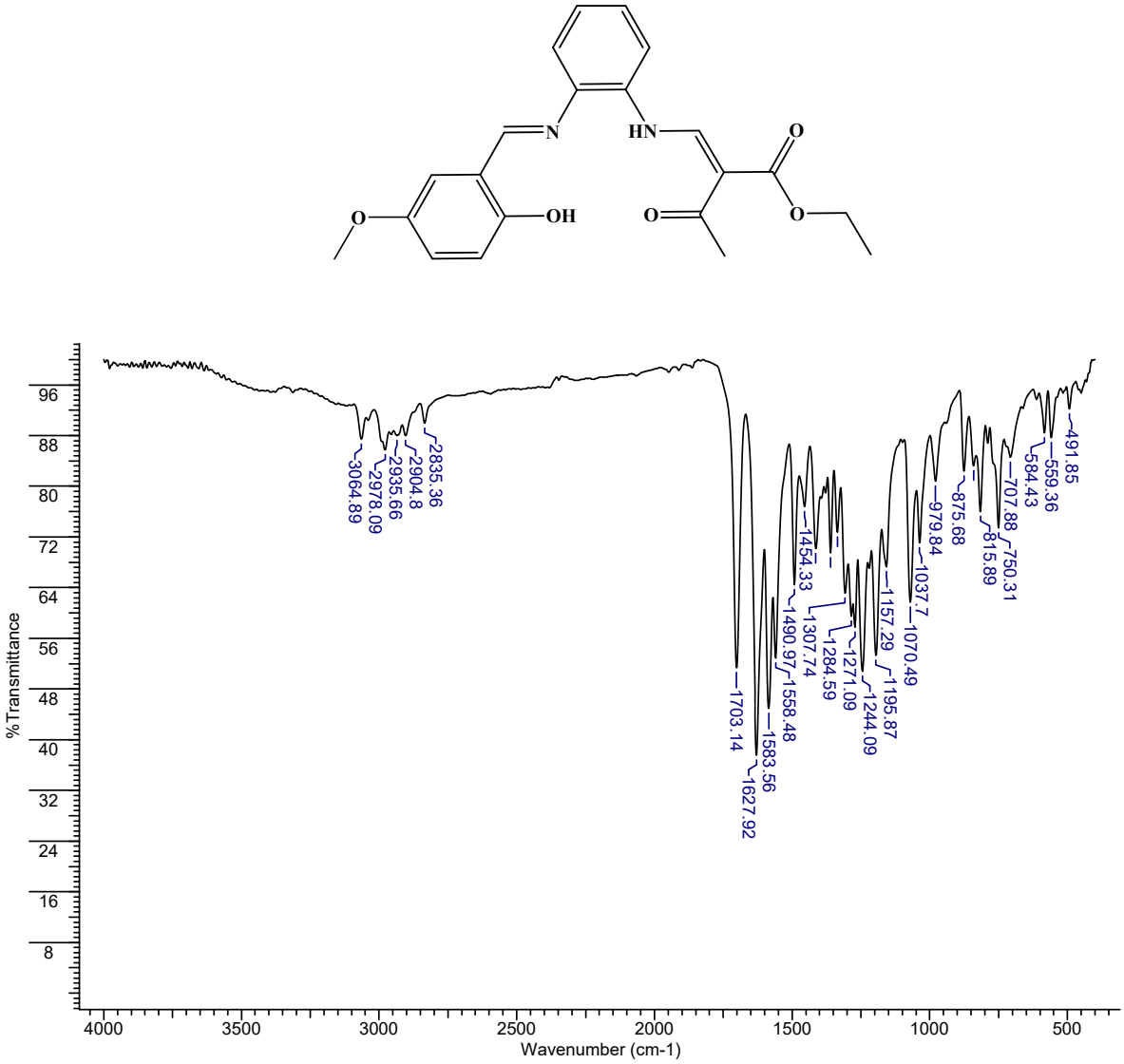

Figure S13. FT-IR spectrum of compound **Ni^{II}-L^1** in KBr disc.

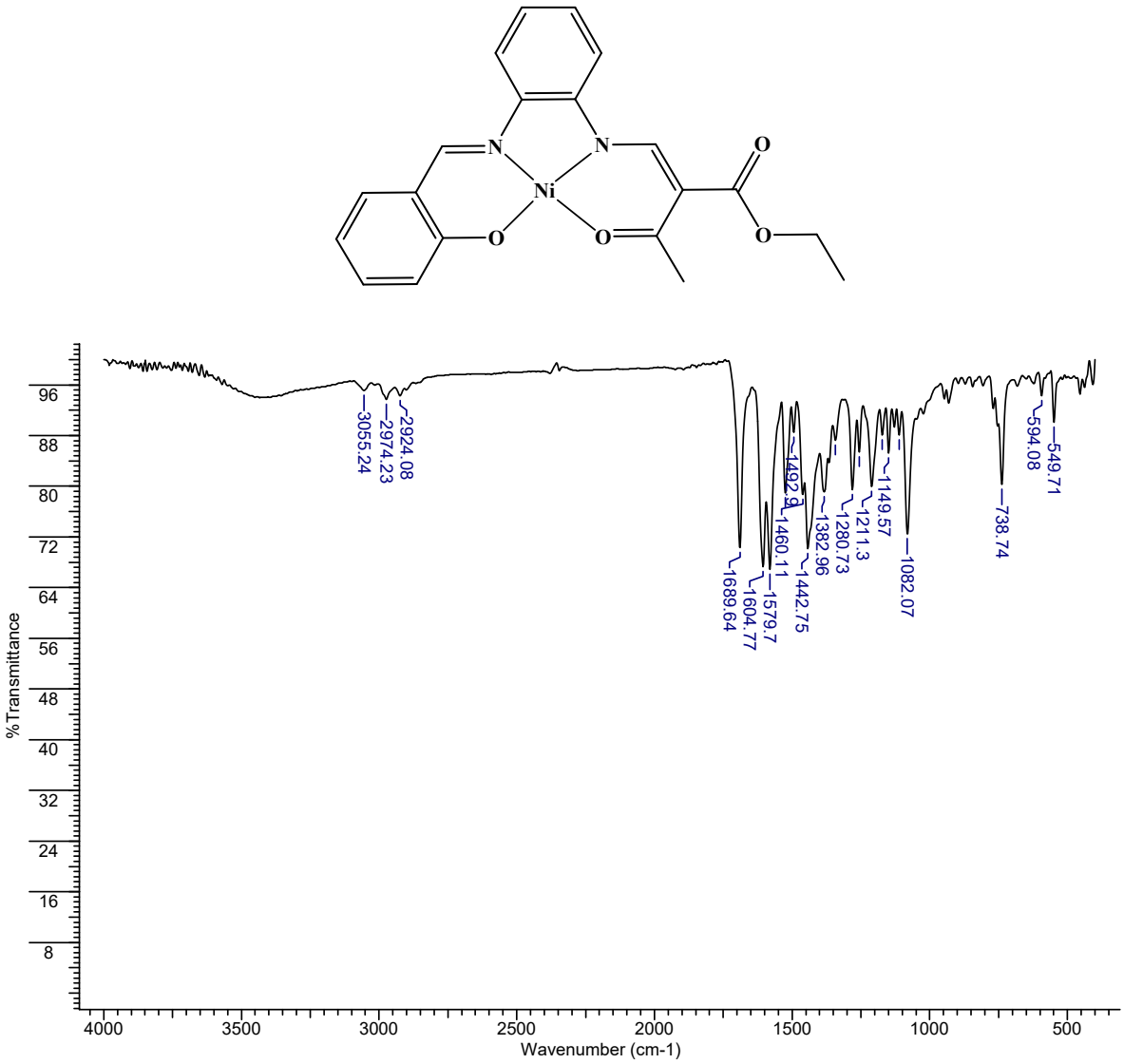

Figure S14. FT-IR spectrum of compound $\mathbf{Zn^{II}\text{-}L^{1}}$ in KBr disc.

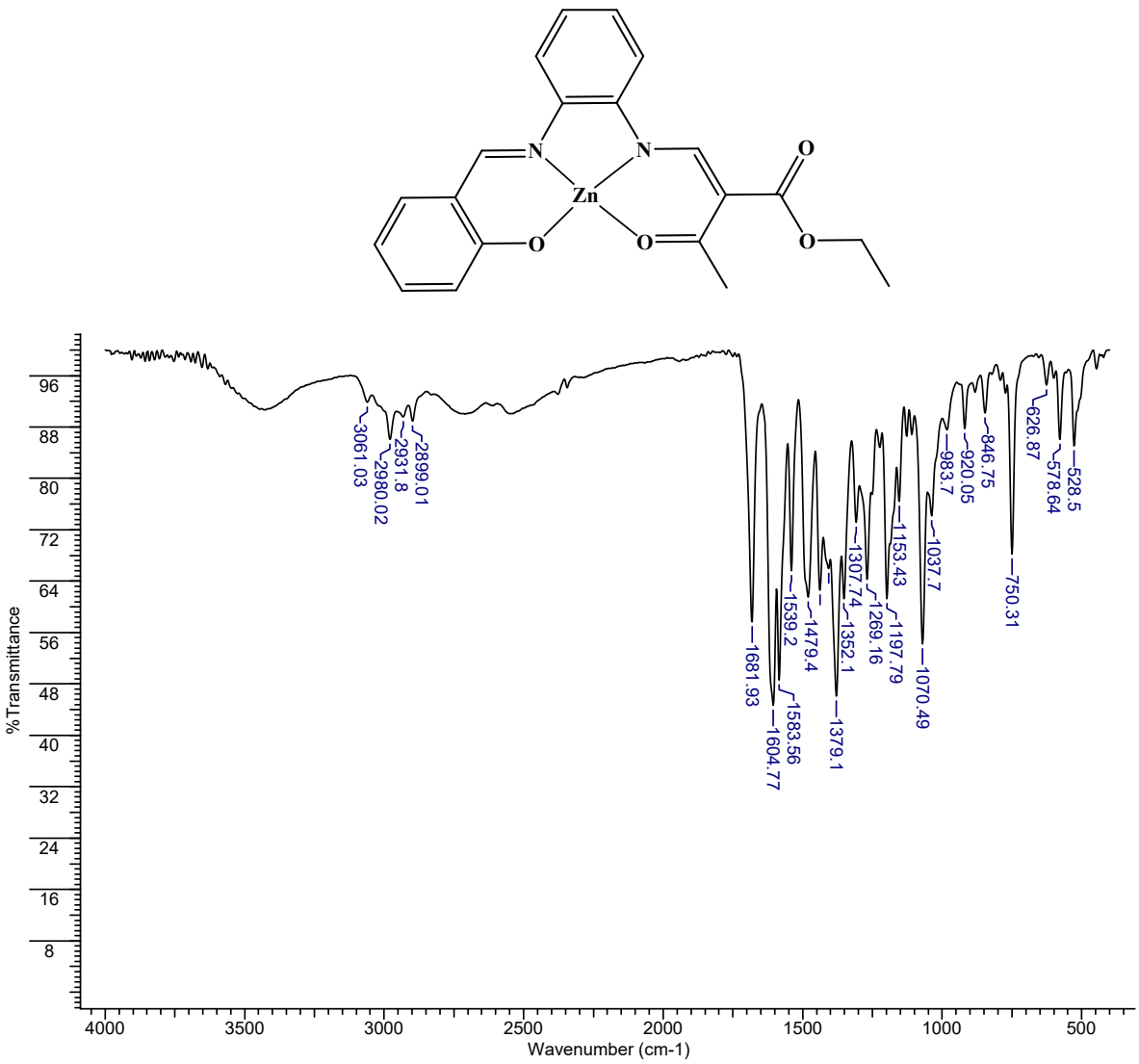

Figure S15. FT-IR spectrum of compound $\mathbf{Ni^{II}\text{-}L^2}$ in KBr disc.

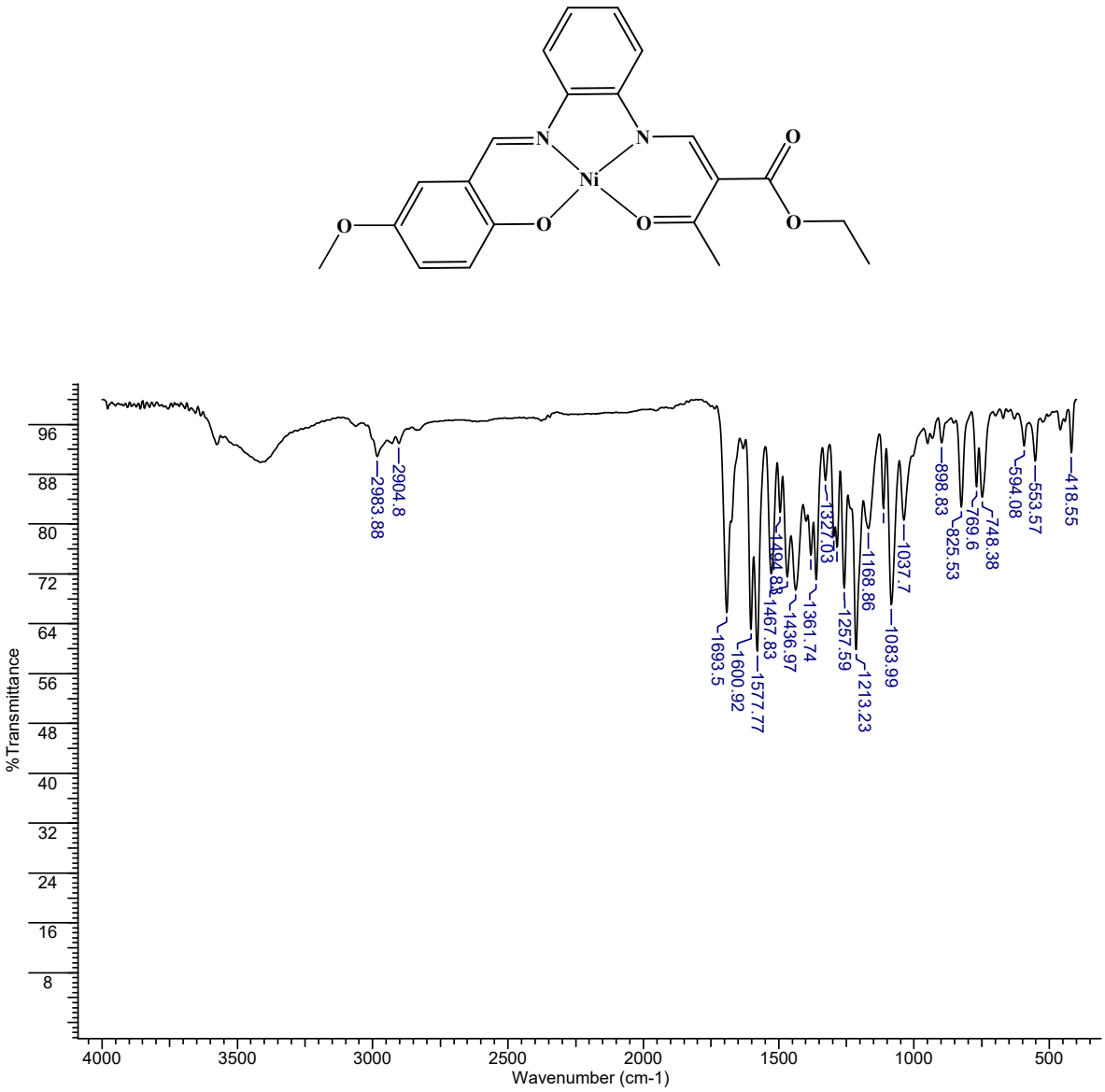

Figure S16. FT-IR spectrum of compound $\mathbf{Zn^{II}\text{-}L^{2}}$ in KBr disc.

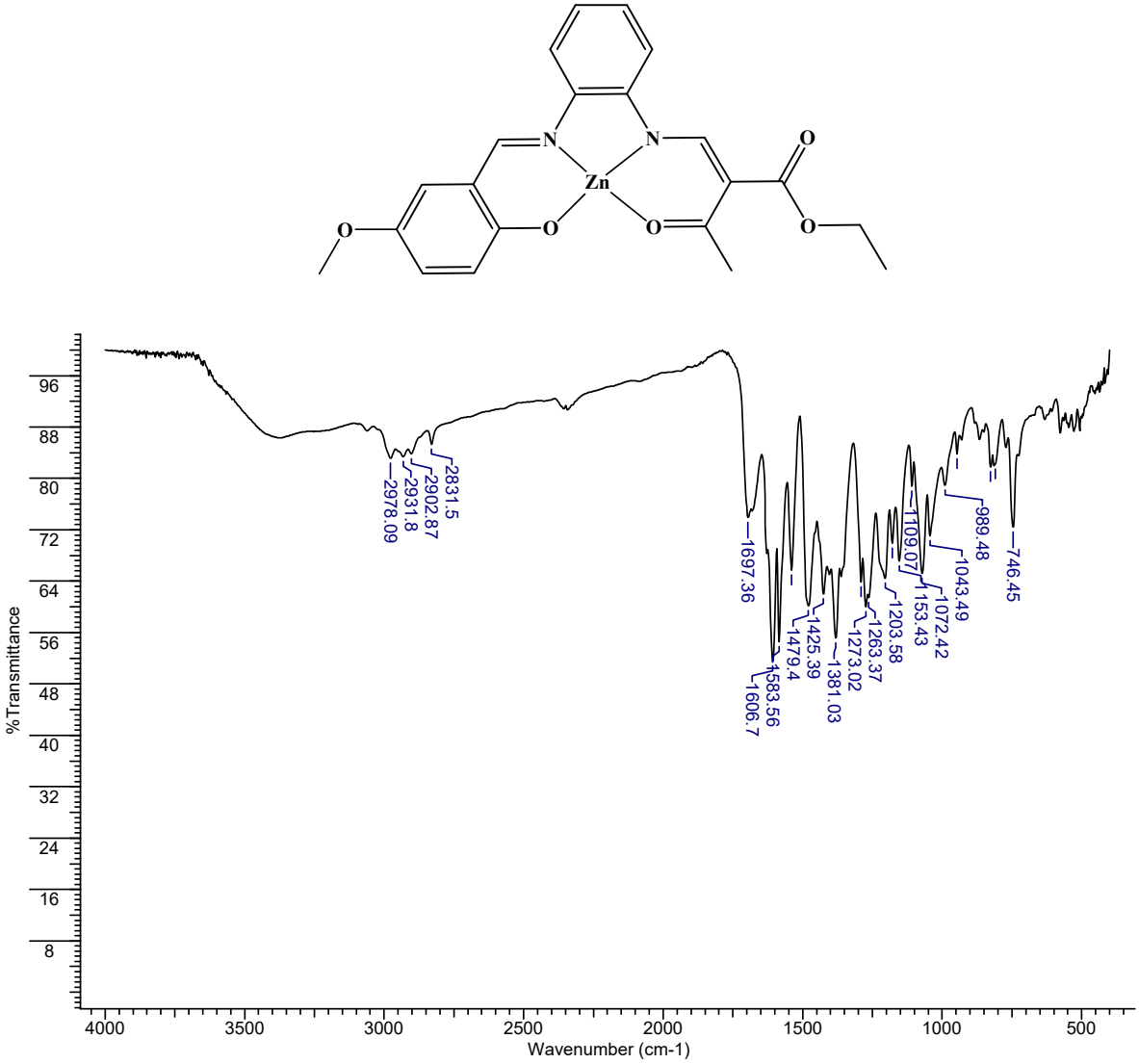

Figure S17. (a) ^{1}H NMR spectrum (400 MHz) of compound $\mathbf{H_2L^1}$ in $CDCl_3$; (b) zoom-in of the aromatic region of the ^{1}H NMR spectrum of $\mathbf{H_2L^1}$.

(a)

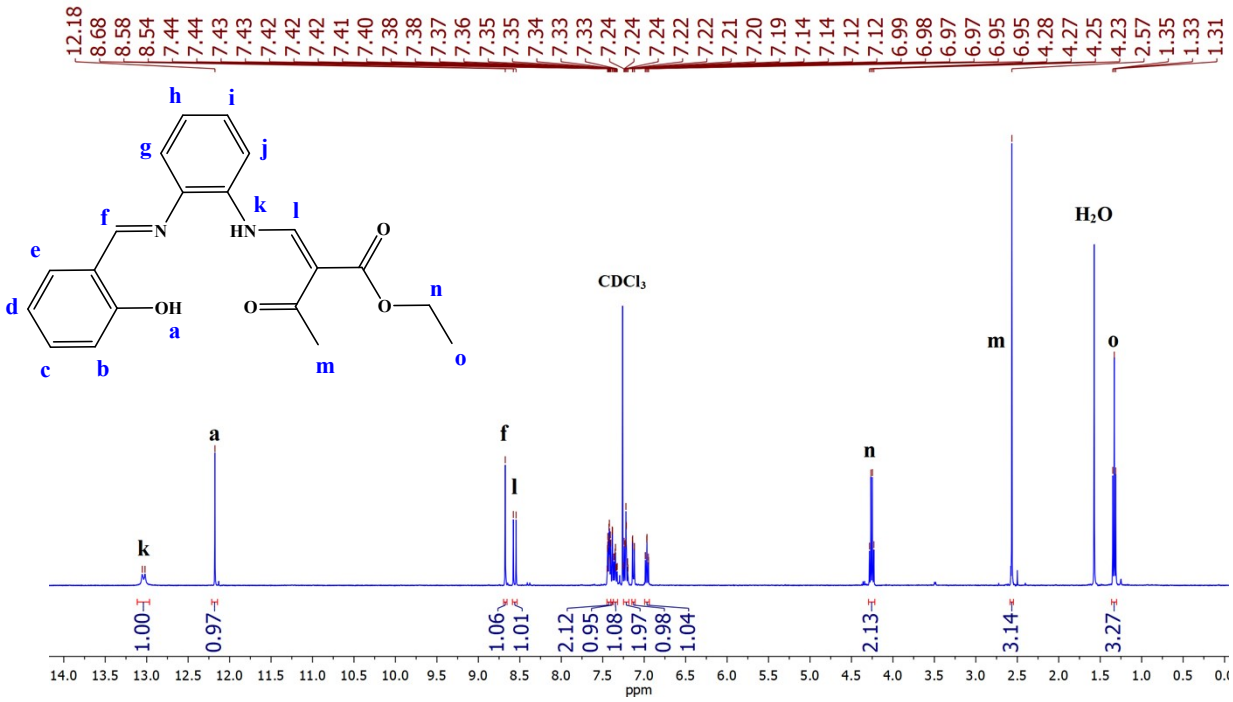

(b)

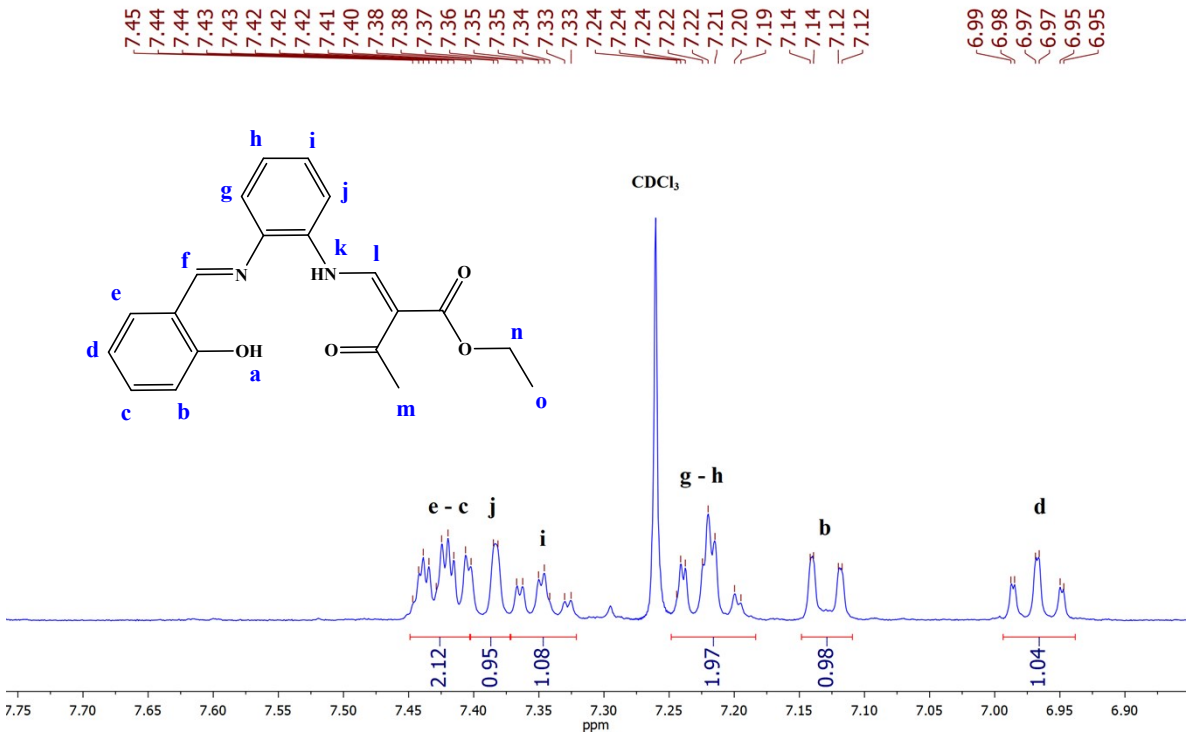
7.45 7.44 7.44 7.43 7.43 7.42 7.42 7.42 7.41 7.40 7.38 7.38 7.37 7.36 7.35 7.35 7.34 7.33 7.33 7.24 7.24 7.24 7.22 7.22 7.21 7.20 7.19 7.14 7.14 7.12 7.12
6.99 6.98 6.97 6.97 6.95 6.95
h i g j f N HN k l O e d OH a c b m O O n o
CDCl3
e - c j i g - h b d
2.12 0.95 1.08 1.97 0.98 1.04
7.75 7.70 7.65 7.60 7.55 7.50 7.45 7.40 7.35 7.30 7.25 7.20 7.15 7.10 7.05 7.00 6.95 6.90
ppm

Figure S18. (a) ^{1}H NMR spectrum (400 MHz) of compound $\mathbf{H_2L^2}$ in $CDCl_3$; (b) zoom-in of the aromatic region of the ^{1}H NMR spectrum of $\mathbf{H_2L^2}$.

(a)

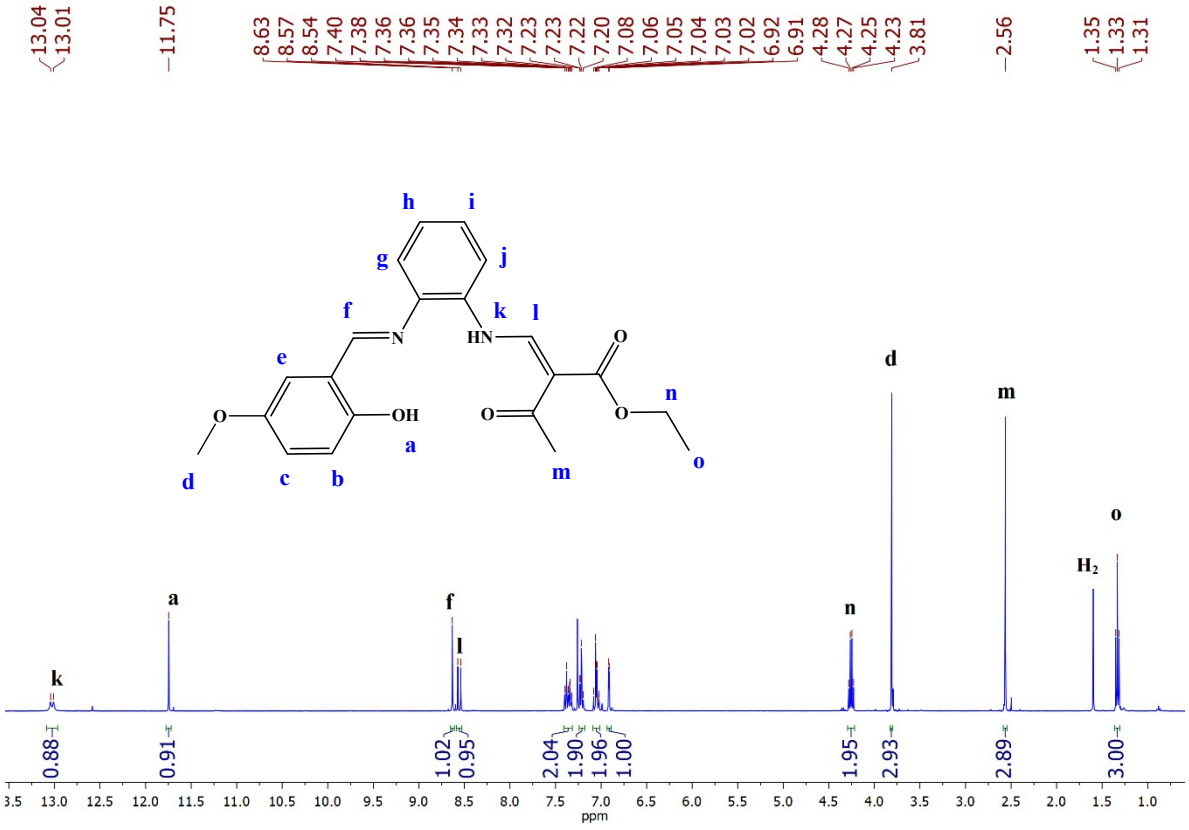

(b)

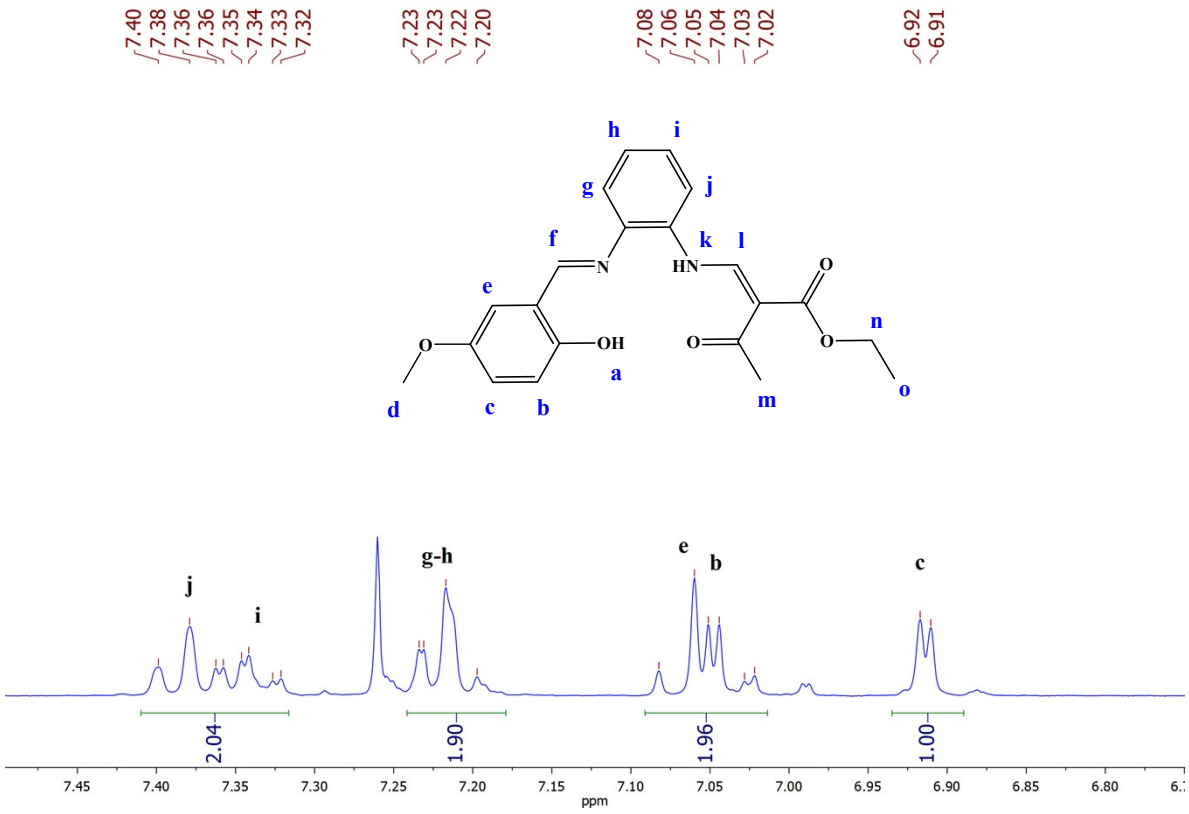
7.40
7.38
7.36
7.36
7.35
7.34
7.33
7.32
7.23
7.23
7.22
7.20
7.08
7.06
7.05
7.04
7.03
7.02
6.92
6.91
h
i
g
j
f
k
l
N
HN
O
e
n
O
OH
O
O
a
d
c
b
m
o
j
i
g-h
e
b
c
2.04
1.90
1.96
1.00
7.45
7.40
7.35
7.30
7.25
7.20
7.15
7.10
7.05
7.00
6.95
6.90
6.85
6.80
ppm

Figure S19. (a) ^{1}H NMR spectrum (400 MHz) of compound **Ni^{II}-L^{1}** in $CDCl_3$; (b) zoom-in of the aromatic region of the ^{1}H NMR spectrum of **Ni^{II}-L^{1}.**

(a)

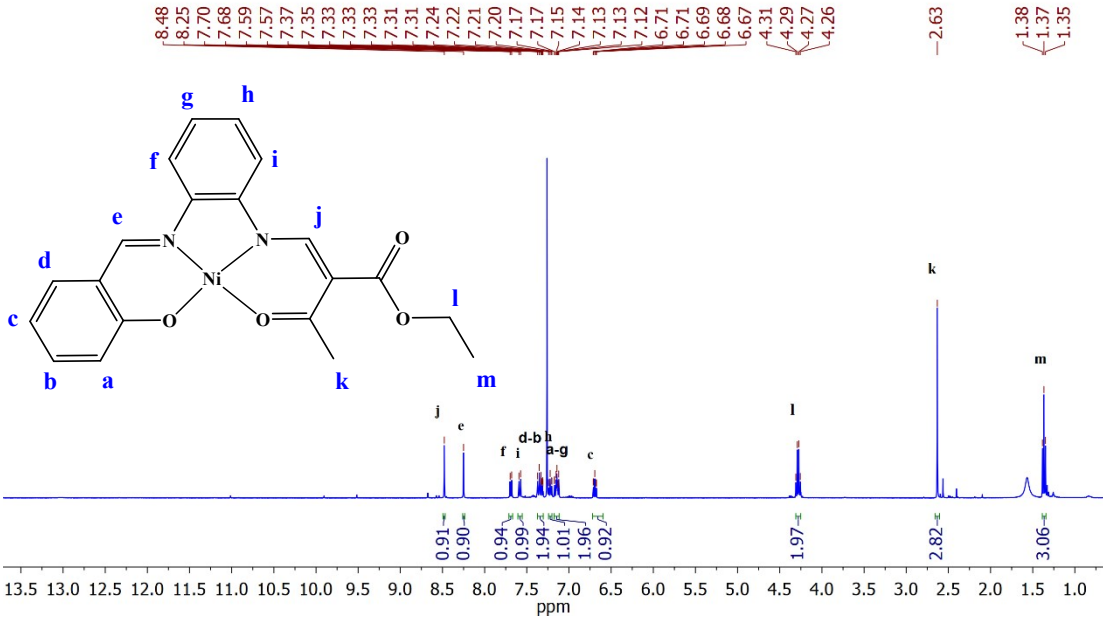

(b)

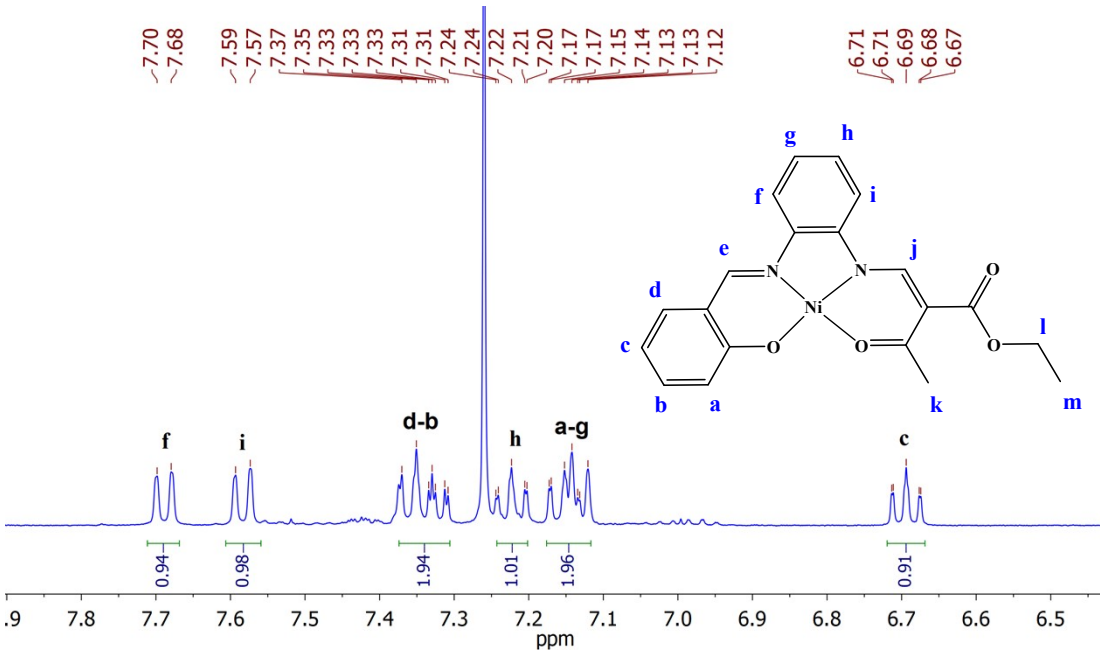
7.70
7.68
7.59
7.57
7.37
7.35
7.33
7.33
7.33
7.31
7.31
7.24
7.24
7.22
7.21
7.20
7.17
7.17
7.15
7.14
7.13
7.13
7.12
6.71
6.71
6.69
6.68
6.67
g
h
f
i
e
j
d
c
b
a
k
l
m
N
N
Ni
O
O
O
O
f
i
d-b
h
a-g
c
0.94
0.98
1.94
1.01
1.96
0.91
.9
7.8
7.7
7.6
7.5
7.4
7.3
7.2
7.1
7.0
6.9
6.8
6.7
6.6
6.5
ppm

Figure S20. (a) ^{1}H NMR spectrum (400 MHz) of compound **Zn^{II}-L^{1}** in DMSO; (b) zoom-in of the aromatic region of the ^{1}H NMR spectrum of **Zn^{II}-L^{1}**

a)

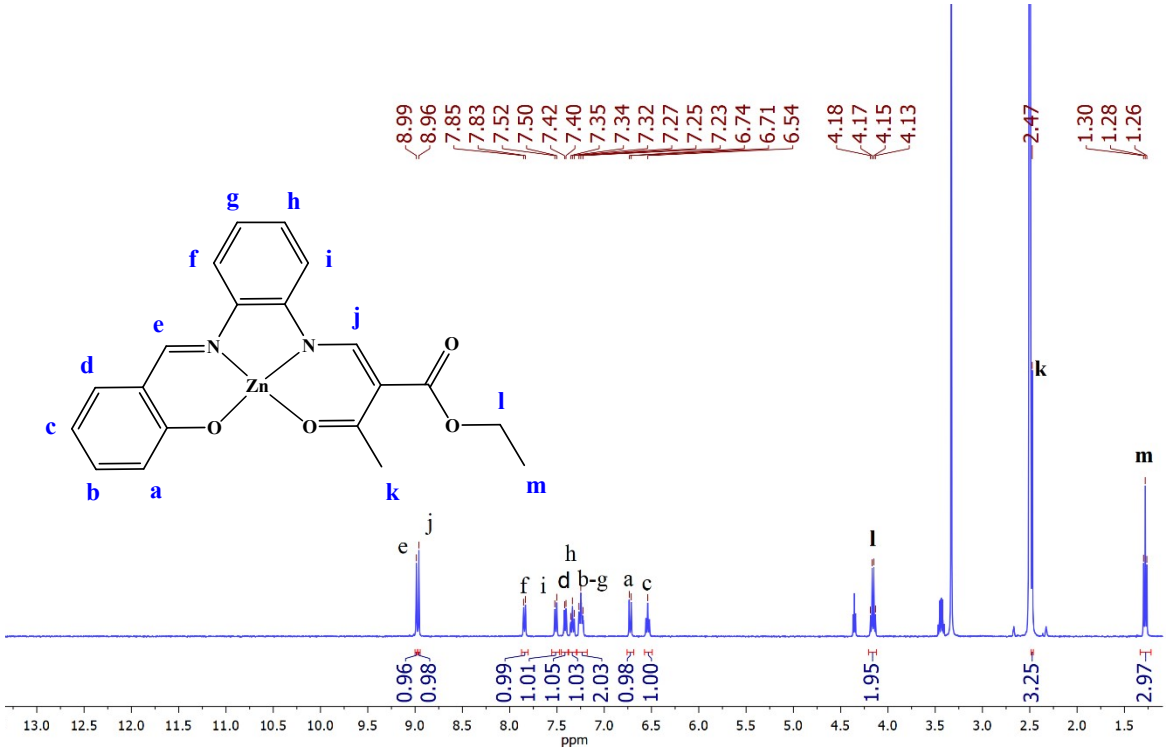

b)

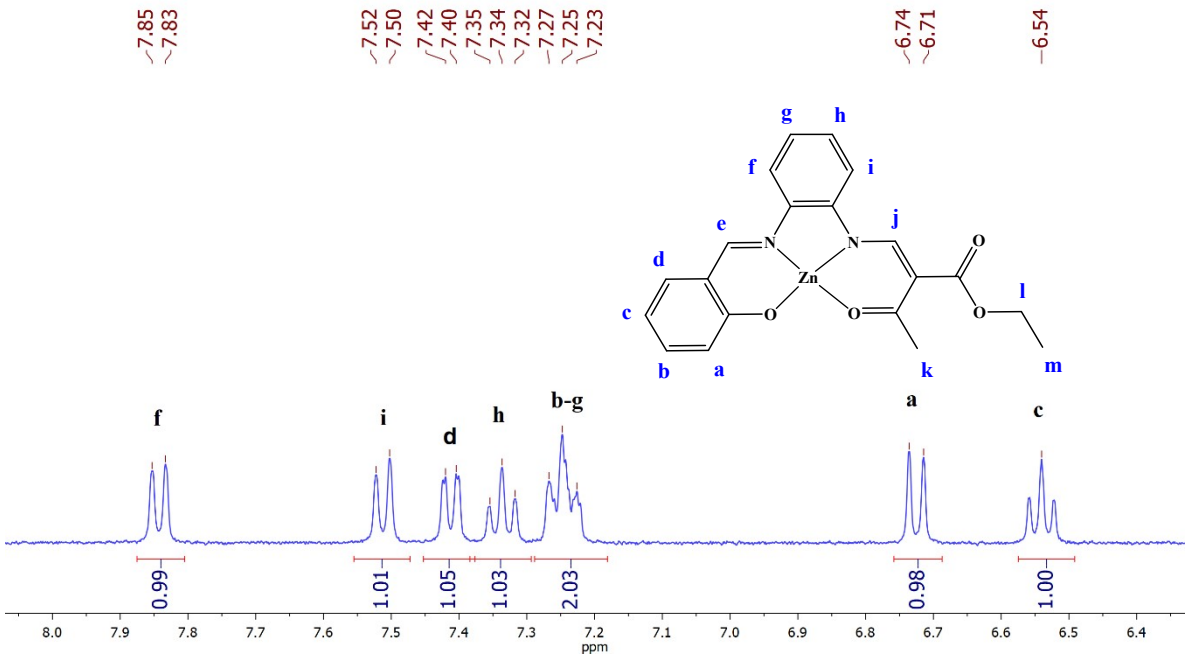
7.85
7.83
7.52
7.50
7.42
7.40
7.35
7.34
7.32
7.27
7.25
7.23
6.74
6.71
6.54
g
h
f
i
e
j
d
c
b
a
k
l
m
Zn
O
N
f
i
d
h
b-g
a
c
0.99
1.01
1.05
1.03
2.03
0.98
1.00
8.0
7.9
7.8
7.7
7.6
7.5
7.4
7.3
7.2
7.1
7.0
6.9
6.8
6.7
6.6
6.5
6.4
ppm

Figure S21. (a) ^{1}H NMR spectrum (400 MHz) of compound **Ni^{II}-L^{2}** in $CDCl_3$; (b) zoom-in of the aromatic region of the ^{1}H NMR spectrum of **Ni^{II}-L^{2}**.

(a)

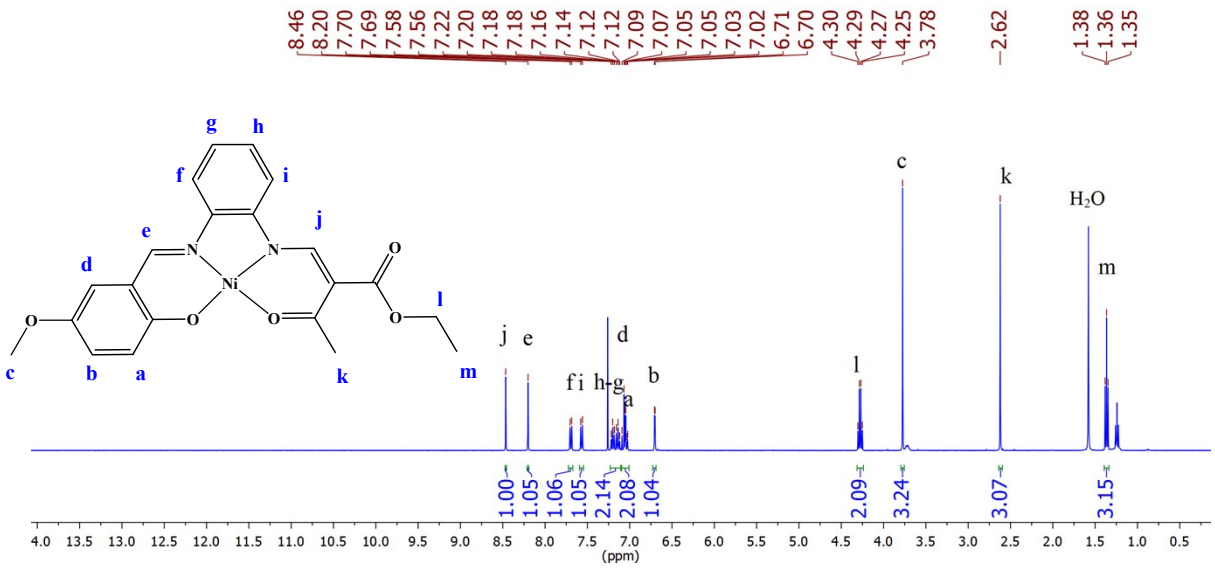

(b)

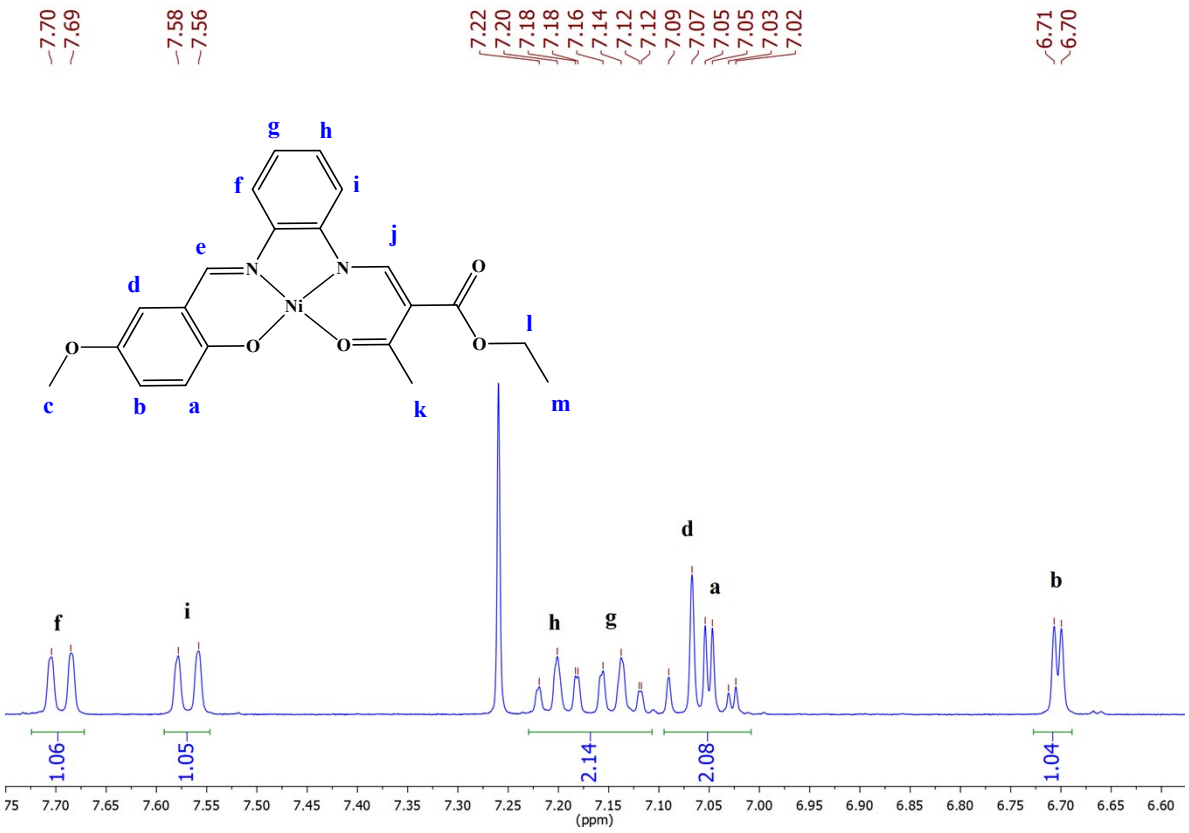
7.70
7.69
7.58
7.56
7.22
7.20
7.18
7.18
7.16
7.14
7.12
7.12
7.09
7.07
7.05
7.05
7.03
7.02
6.71
6.70
g
h
f
i
e
j
d
N
N
Ni
O
O
O
O
O
l
c
b
a
k
m
d
a
b
f
i
h
g
1.06
1.05
2.14
2.08
1.04
7.75
7.70
7.65
7.60
7.55
7.50
7.45
7.40
7.35
7.30
7.25
7.20
7.15
7.10
7.05
7.00
6.95
6.90
6.85
6.80
6.75
6.70
6.65
6.60
(ppm)

Figure S22. (a) ^{1}H NMR spectrum (400 MHz) of compound **Zn^{II}-L^{2}** in DMSO; (b) zoom-in of the aromatic region of the ^{1}H NMR spectrum of **Zn^{II}-L^{2}**.

(a)

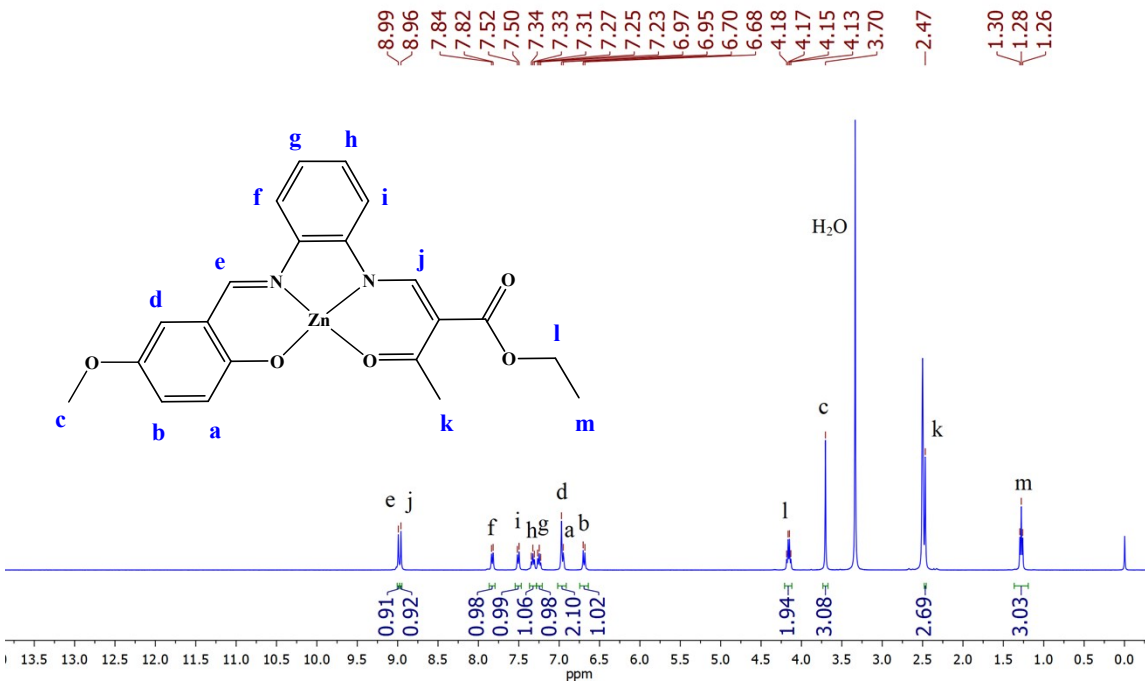

(b)

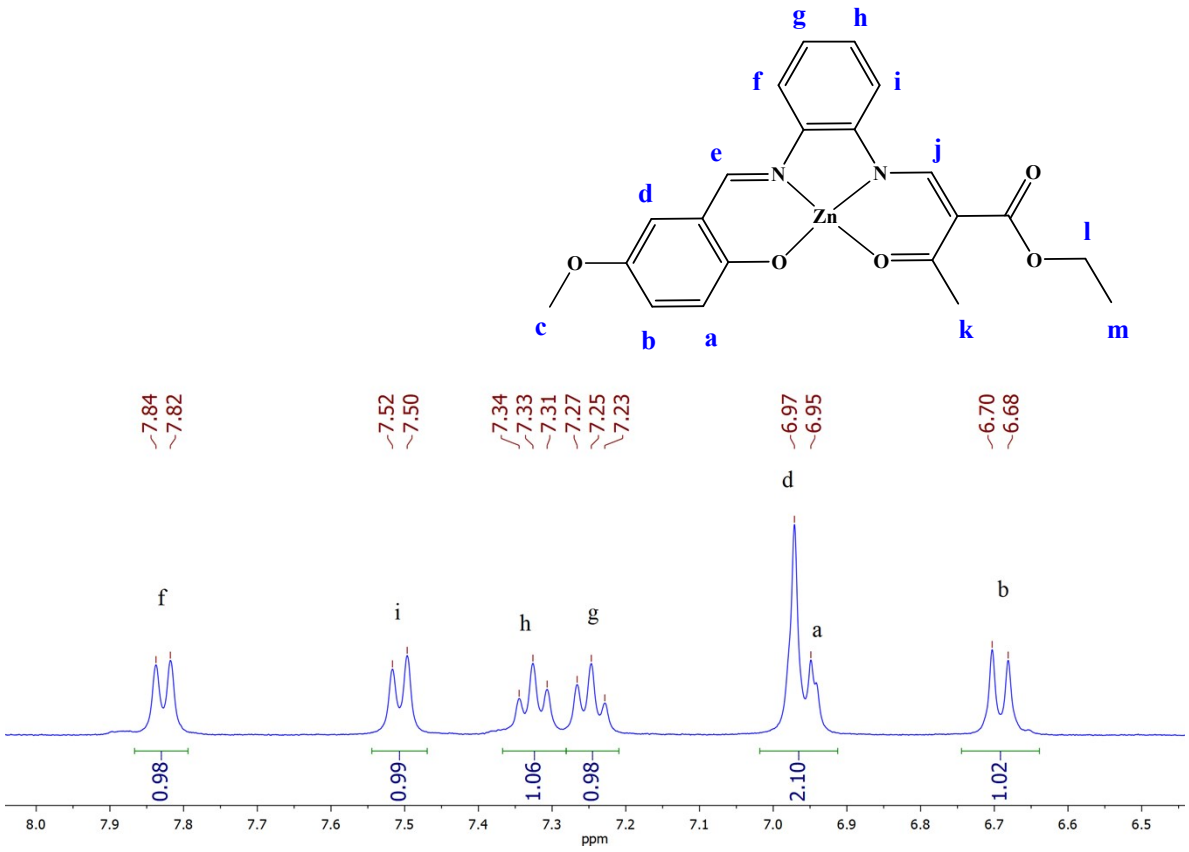
g
h
f
i
e
j
d
N
N
Zn
O
O
O
O
O
l
c
b
a
k
m
7.84
7.82
7.52
7.50
7.34
7.33
7.31
7.27
7.25
7.23
6.97
6.95
6.70
6.68
d
f
i
h
g
a
b
0.98
0.99
1.06
0.98
2.10
1.02
8.0
7.9
7.8
7.7
7.6
7.5
7.4
7.3
7.2
7.1
7.0
6.9
6.8
6.7
6.6
6.5
ppm

Figure S23. ^{13}C NMR spectrum (400 MHz) of compound $\mathbf{H_2L^1}$ in $CDCl_3$.

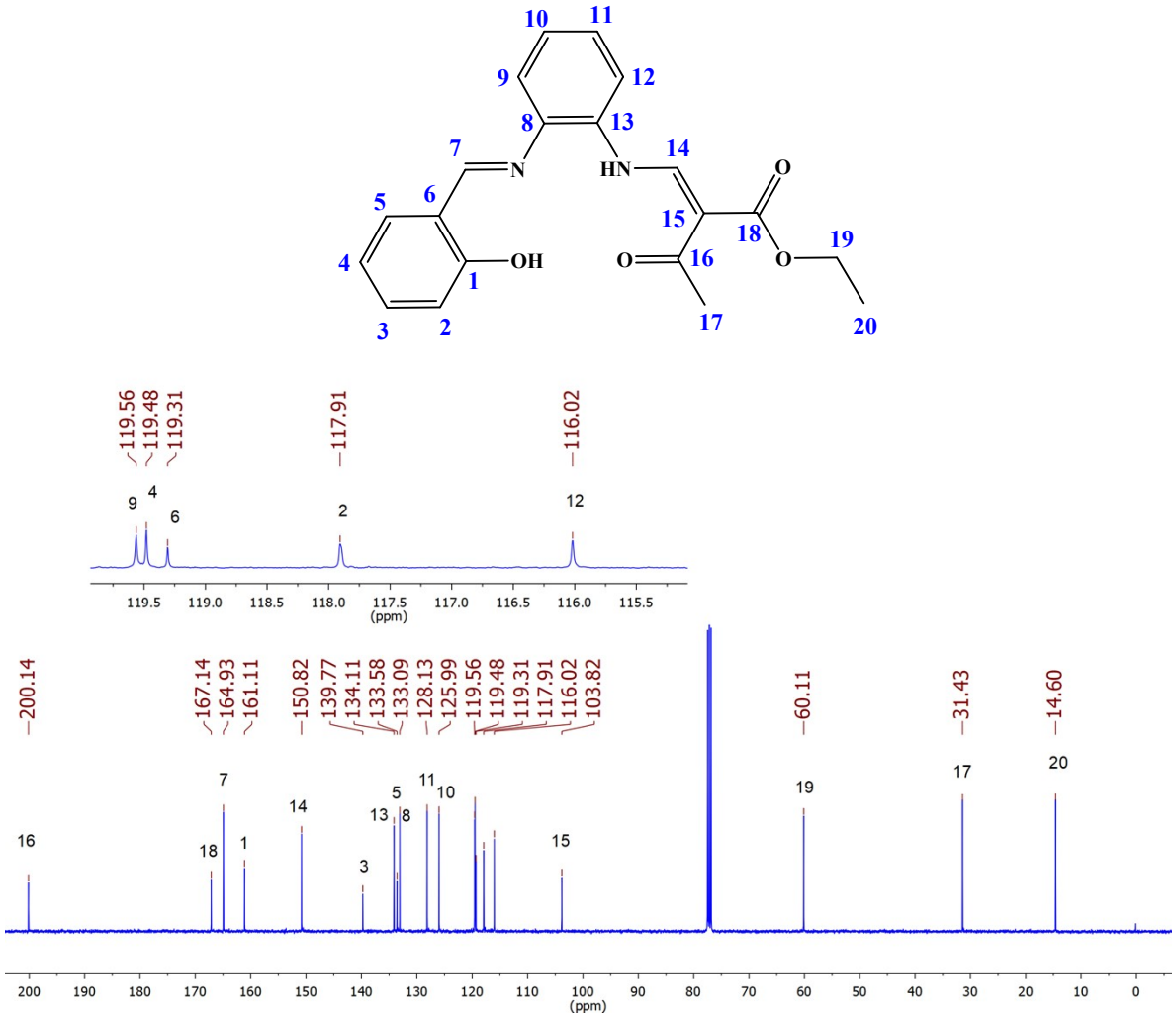

Figure S24. ^{13}C NMR spectrum (400 MHz) of compound $\mathbf{H_2L^2}$ in $CDCl_3$.

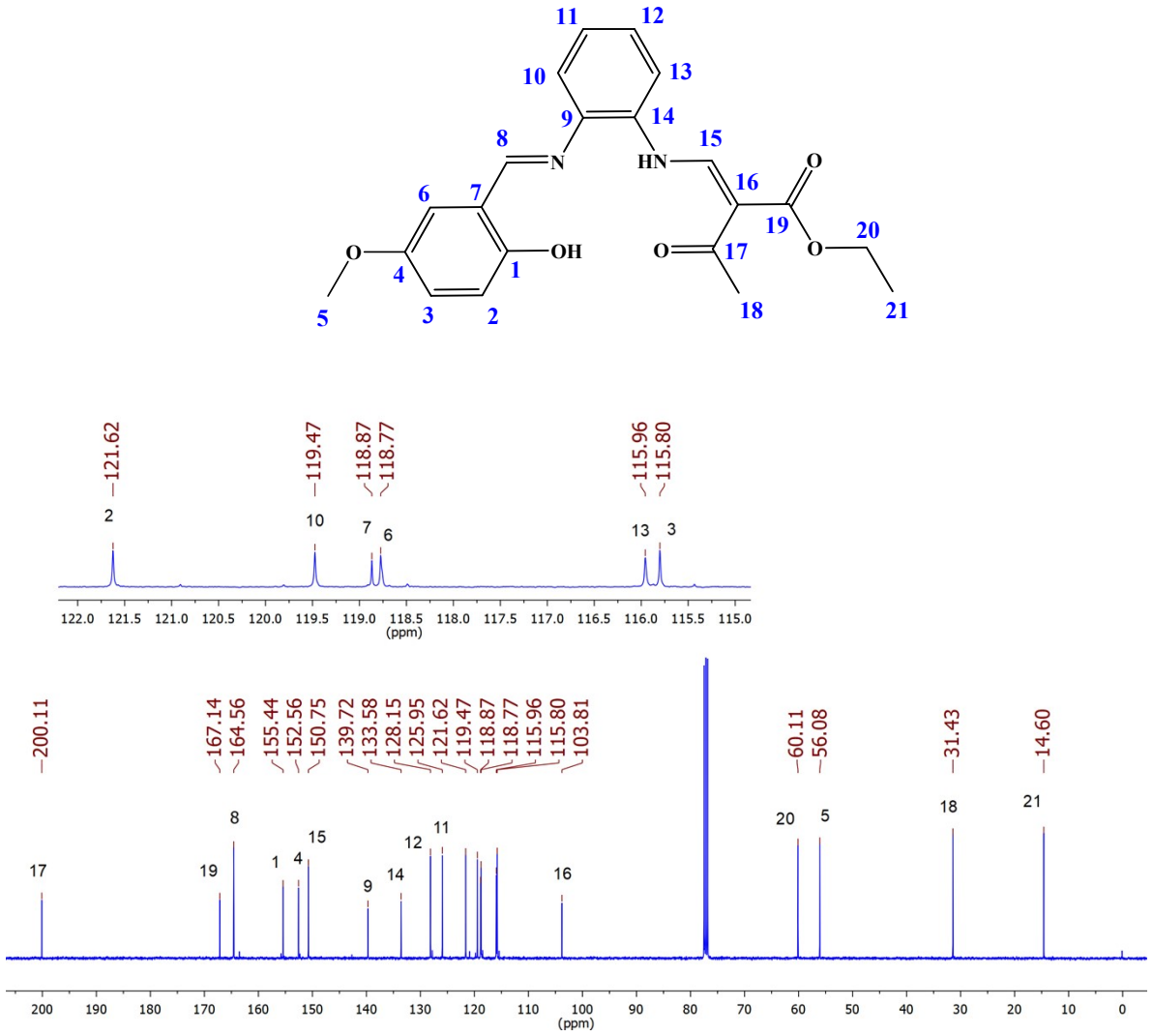

Figure S25. ^{13}C NMR spectrum (400 MHz) of compound **Ni^{II}-L^1** in $CDCl_3$.

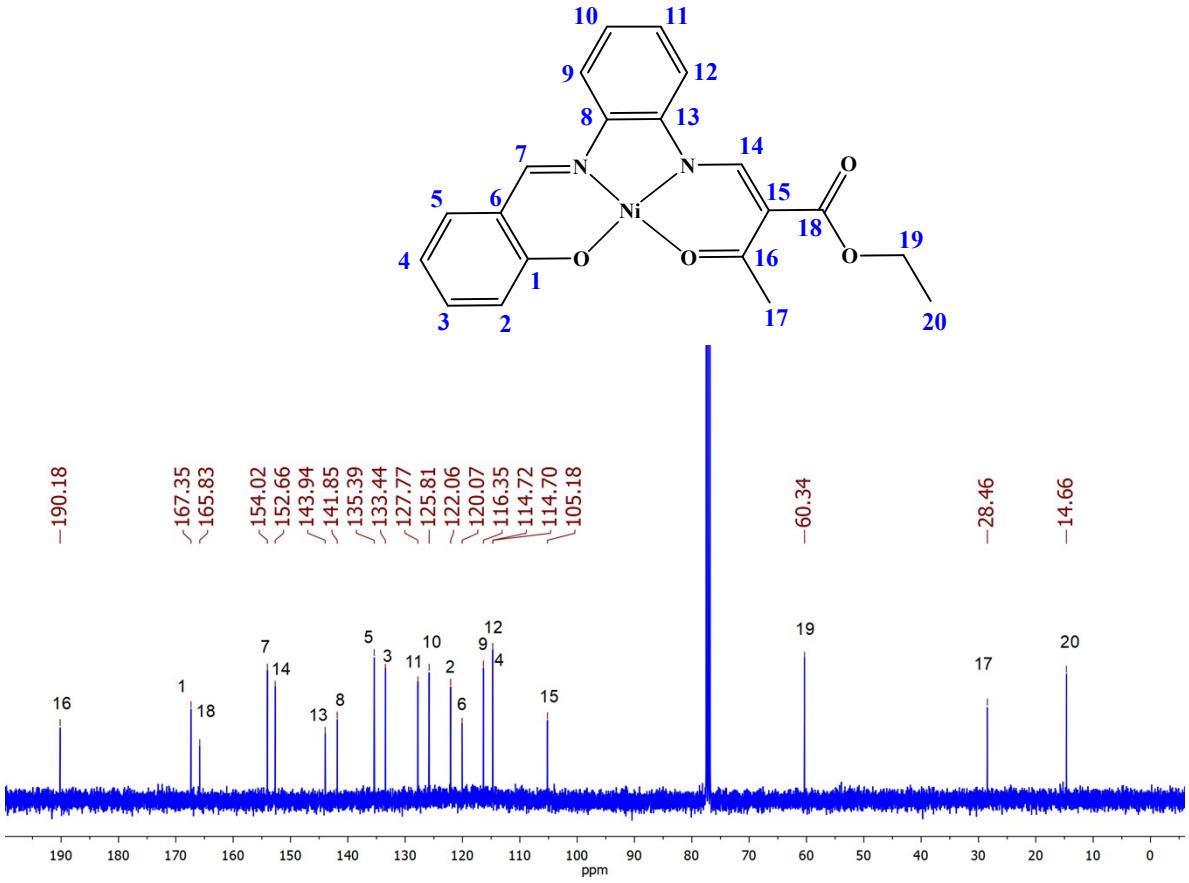

Figure S26. ^{13}C NMR spectrum (400 MHz) of compound **Zn^{II}-L^1** in DMSO.

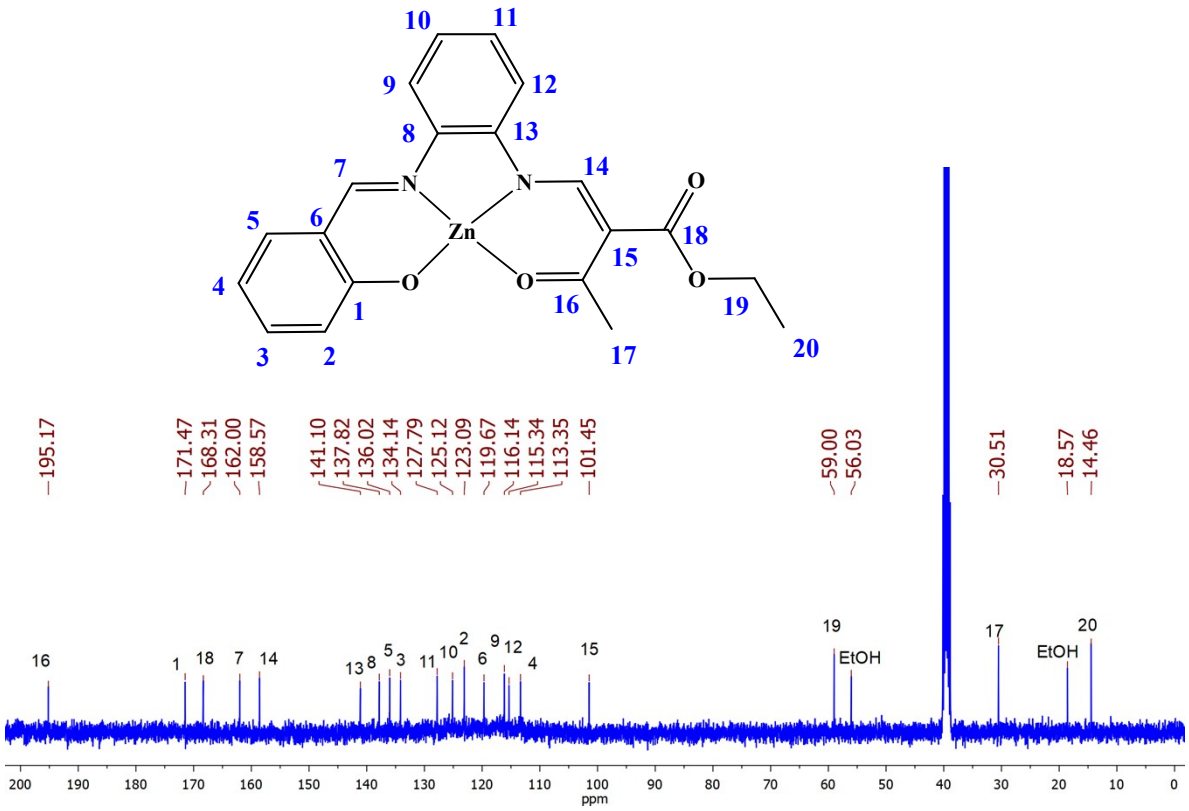

Figure S27. ^{13}C NMR spectrum (400 MHz) of compound **Ni^{II}-L^2** in $CDCl_3$.

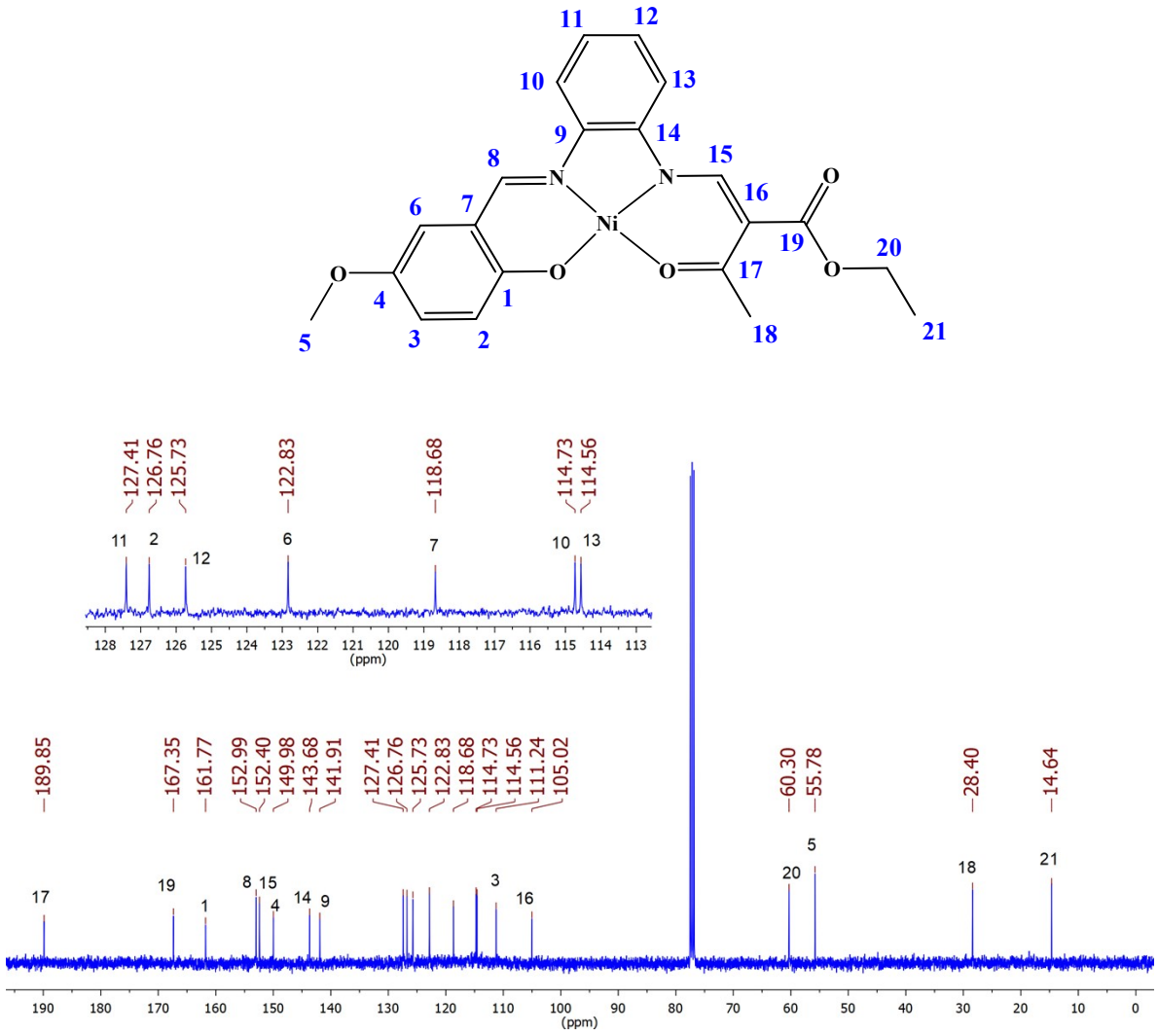

Figure S28. ^{13}C NMR spectrum (400 MHz) of compound **Zn^{II}-L^2** in DMSO.

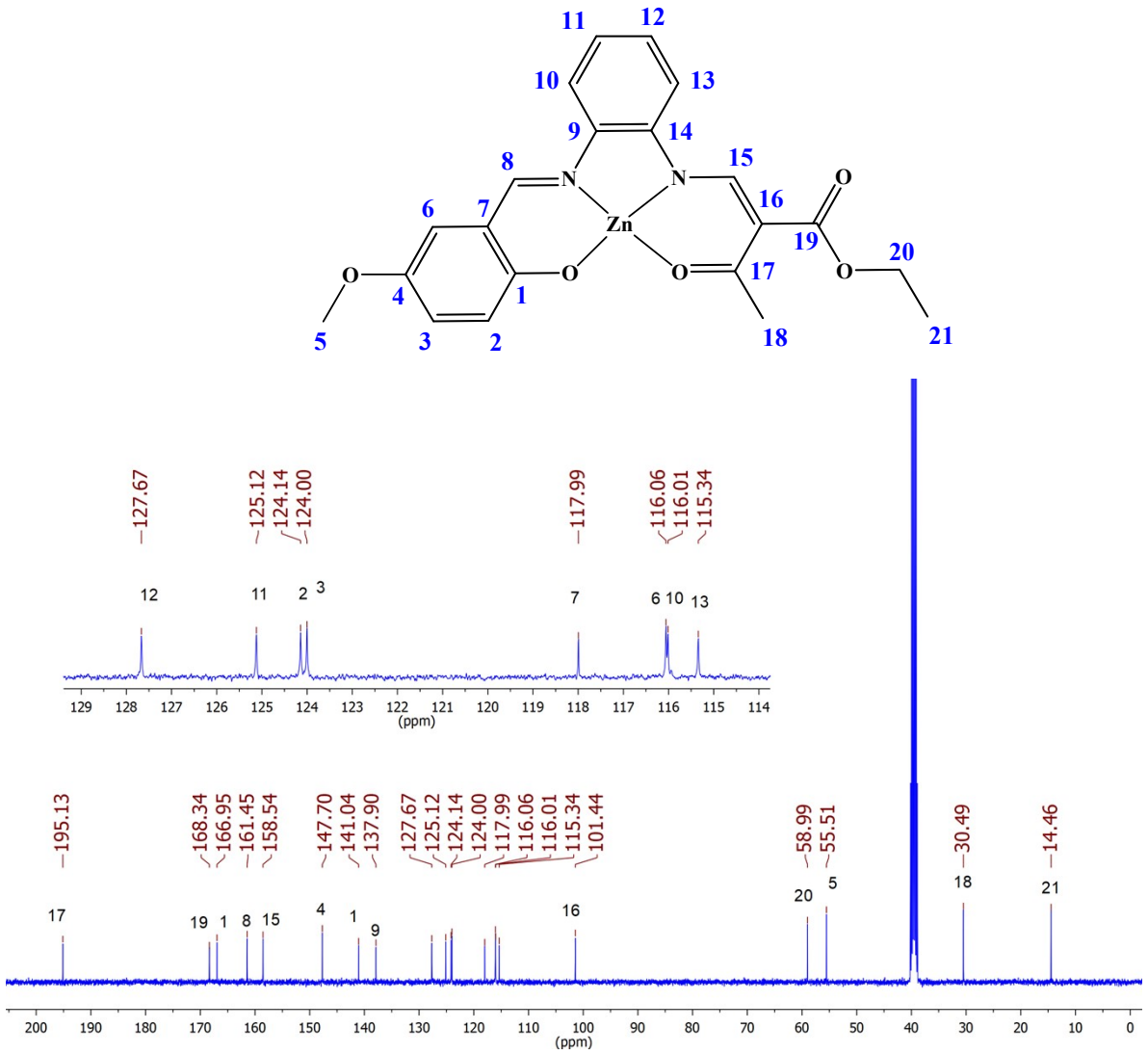

Figure S29. [^{1}H-^{1}H] NOESY NMR spectrum (400 MHz) of compound **Ni^{II}-L^{1}** in $CDCl_3$. The NOESY spectrum of **Ni^{II}-L^{1}** shows the interaction between hydrogen at 8.19 ppm with two hydrogens atoms from aromatic region which is consistent with the assignation of the signal at 8.19 as imine group (CH=N).

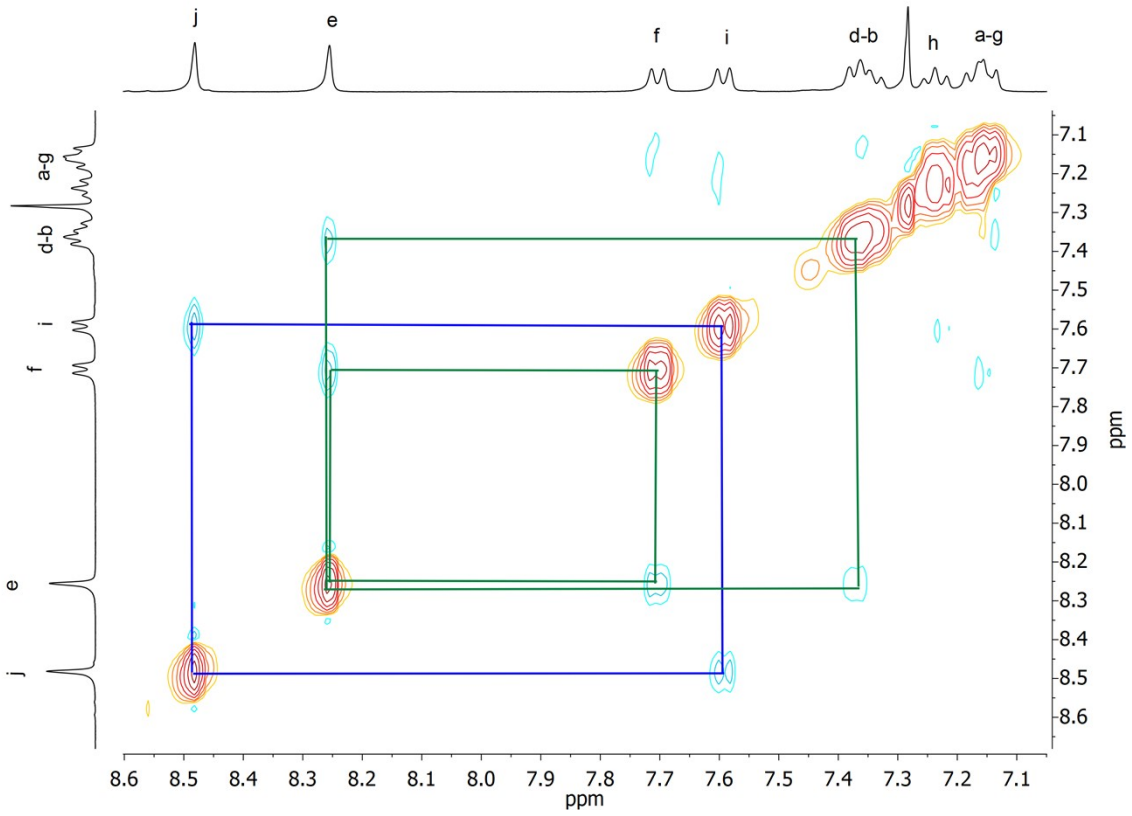

Figure S30. ^{1}H NMR spectra of compound $\mathbf{H_2L^1}$ at different periods of storage (0, 4, 12 and 24 h) in DMSO-d_6:D_2O solution (9:1) at 300 K.

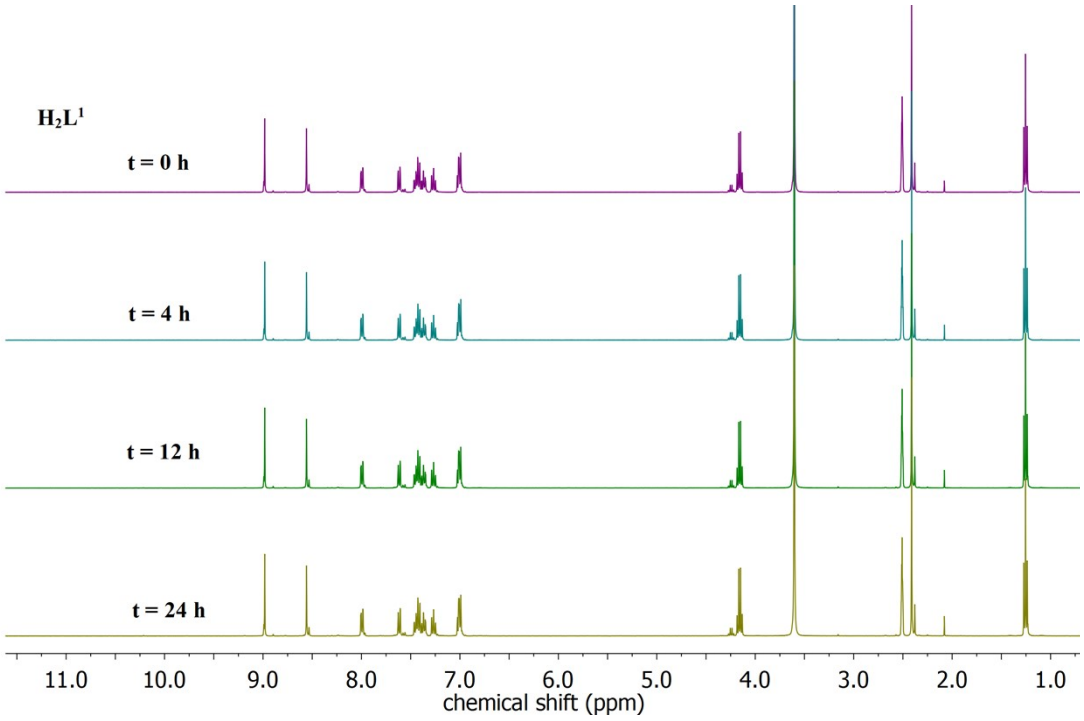

Figure S31. [1]H NMR spectra of compound **H_2L^2** at different periods of storage (0, 4, 12 and 24 h) in DMSO-d_6:D_2O solution (9:1) at 300 K.

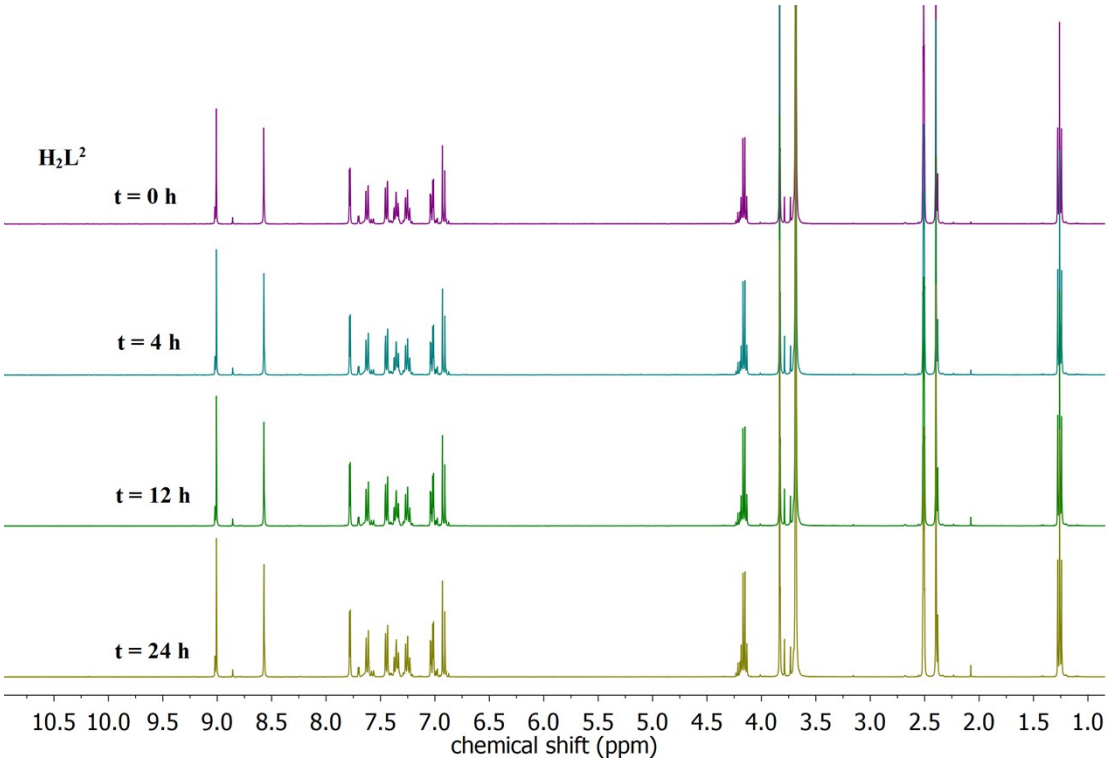

Figure S32. ^{1}H NMR spectra of compound **Ni^{II}-L^{1}** at different periods of storage (0, 4, 12, and 24 h) in DMSO-d_6:D_2O solution (9:1) at 300 K.

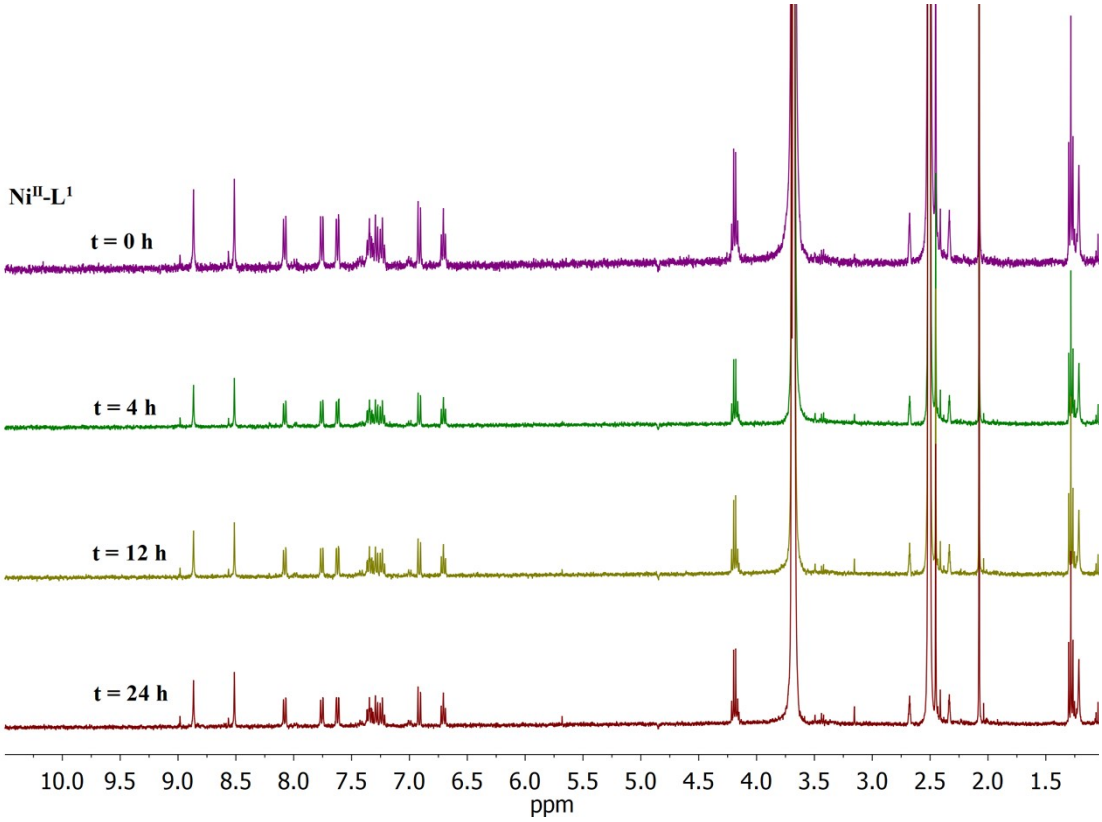

Figure S33. ^{1}H NMR spectra of compound **Zn^{II}-L^{1}** at different periods of storage (0, 4, 12 and 24 h) in DMSO-d_6:D_2O solution (9:1) at 300 K.

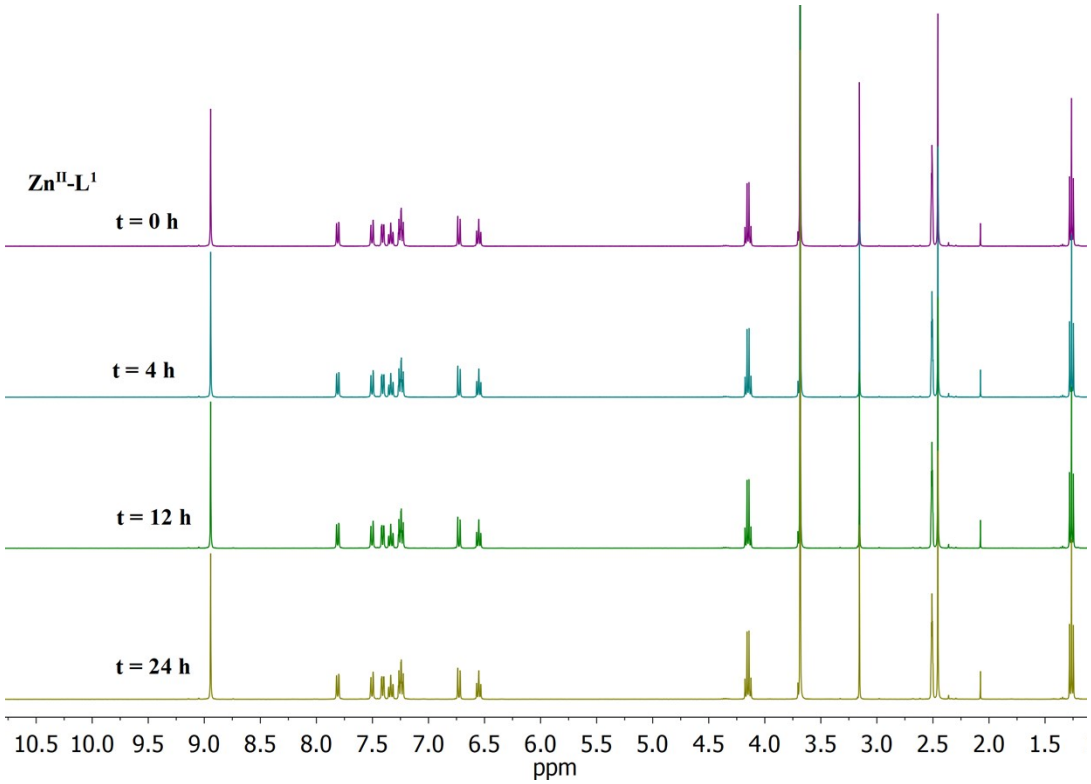

Figure S34. ^{1}H NMR spectra of compound **Ni^{II}-L^{2}** at different periods of storage (0, 4, 12 and 24 h) in DMSO-d_6:D_2O solution (9:1) at 300 K.

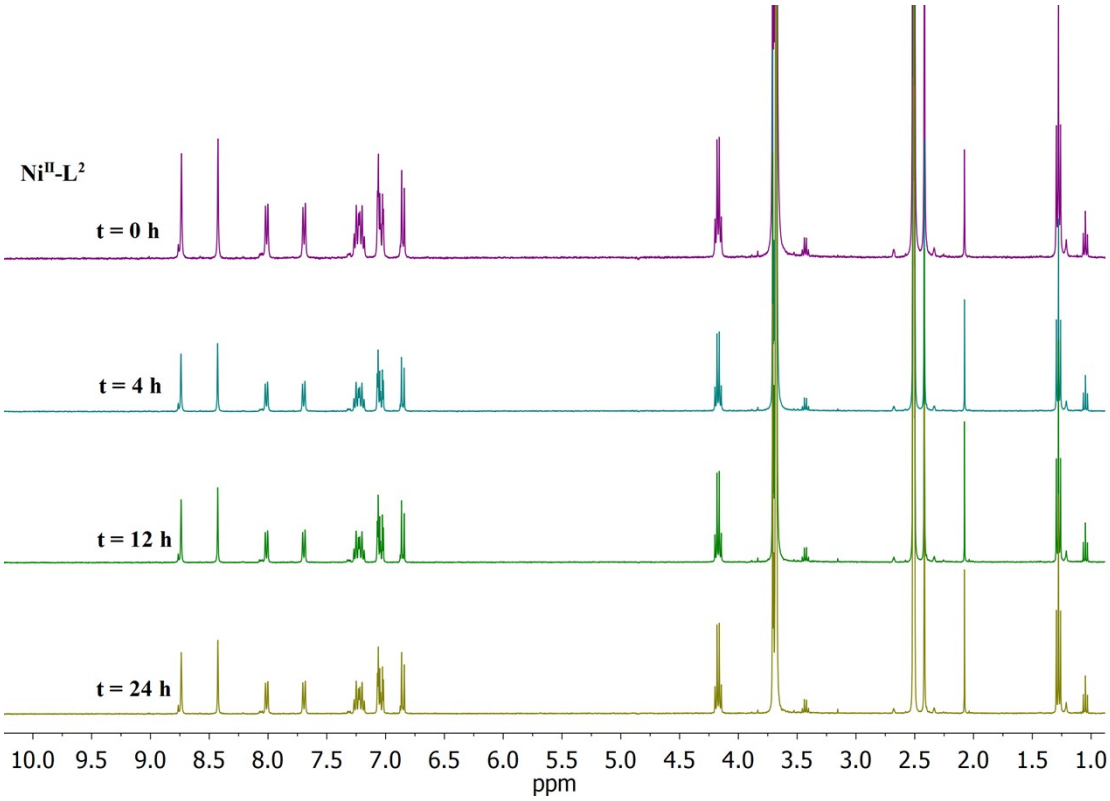

Figure S35. ^{1}H NMR spectra of compound **Zn^{II}-L^{2}** at different periods of storage (0, 4, 12, and 24 h) in DMSO-d_6:D_2O solution (9:1) at 300 K.

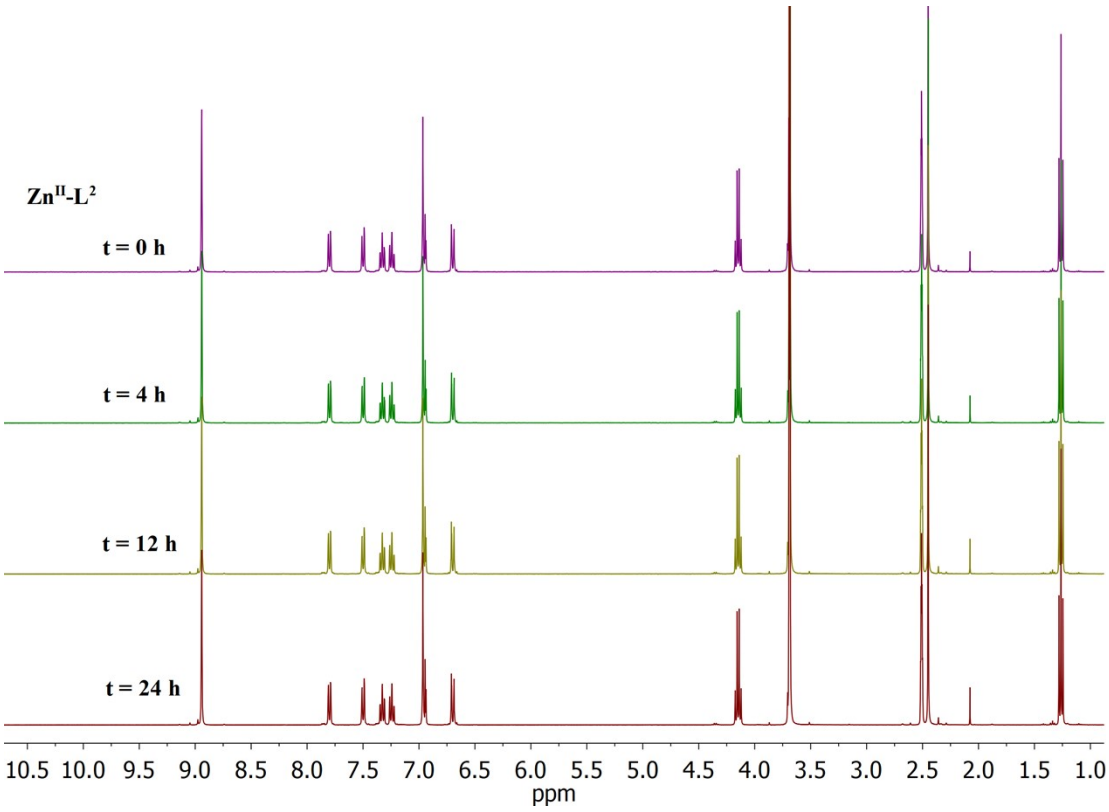

Figure S36. The absorption spectrum of a freshly prepared solution of **Ni^{II}-L_1** in a DMSO:Buffer solution (60:40) and absorption spectral changes after several storage periods. **A)** Contains spectra registered every 3 h, up to 24 h, and in order to ease the visualization, **B)** contains a selection of the spectra obtained for t = 0, 12, and 24 h.

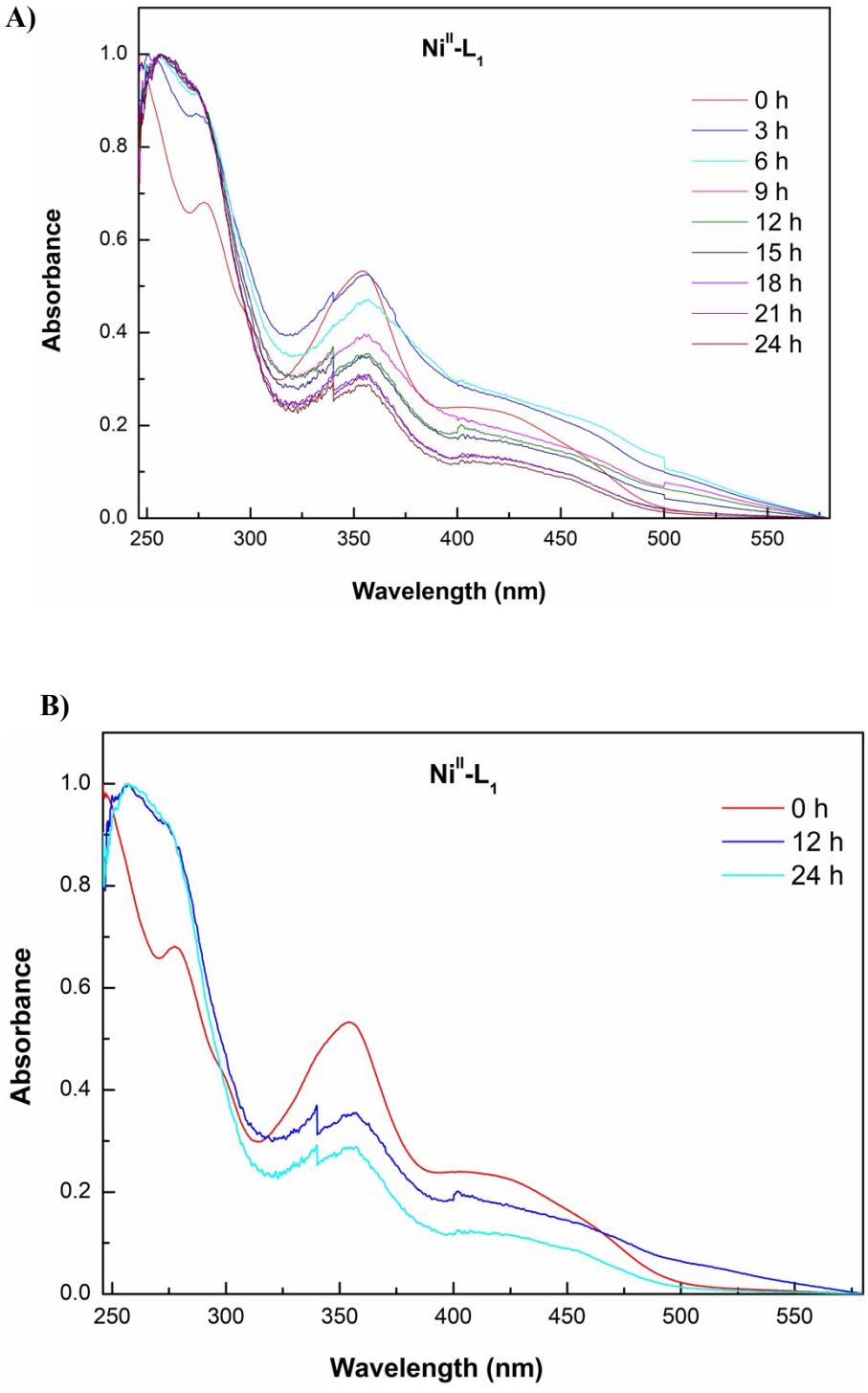

Figure S37. The absorption spectrum of a freshly prepared solution of $\mathbf{Ni^{II}\text{-}L_2}$ in a DMSO:Buffer solution (60:40) and absorption spectral changes after several storage periods. **A)** Contains spectra registered every 3 h, up to 24 h, and in order to ease the visualization, **B)** contains a selection of the spectra obtained for t = 0, 12, and 24 h.

A)

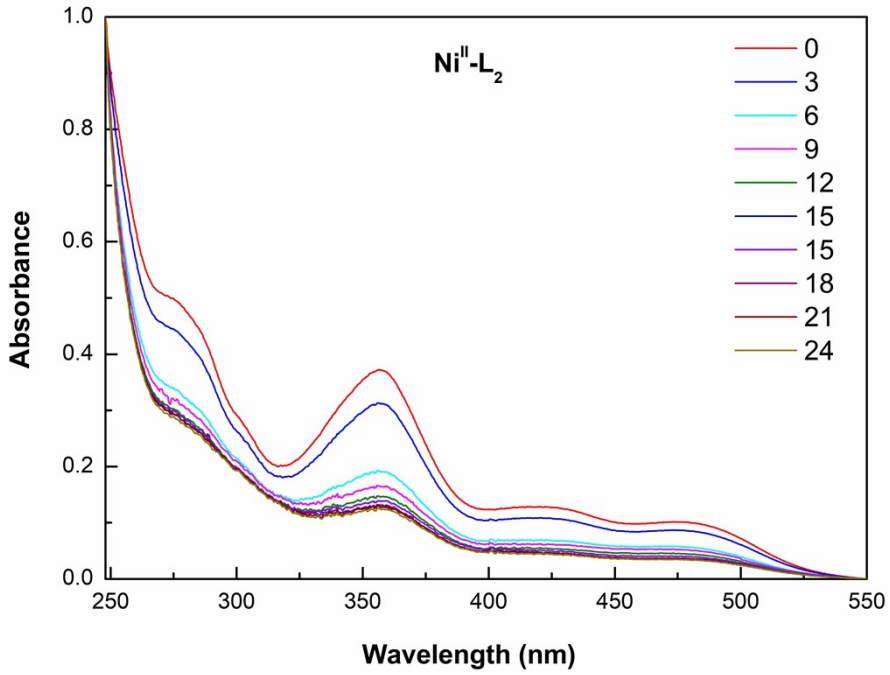

B)

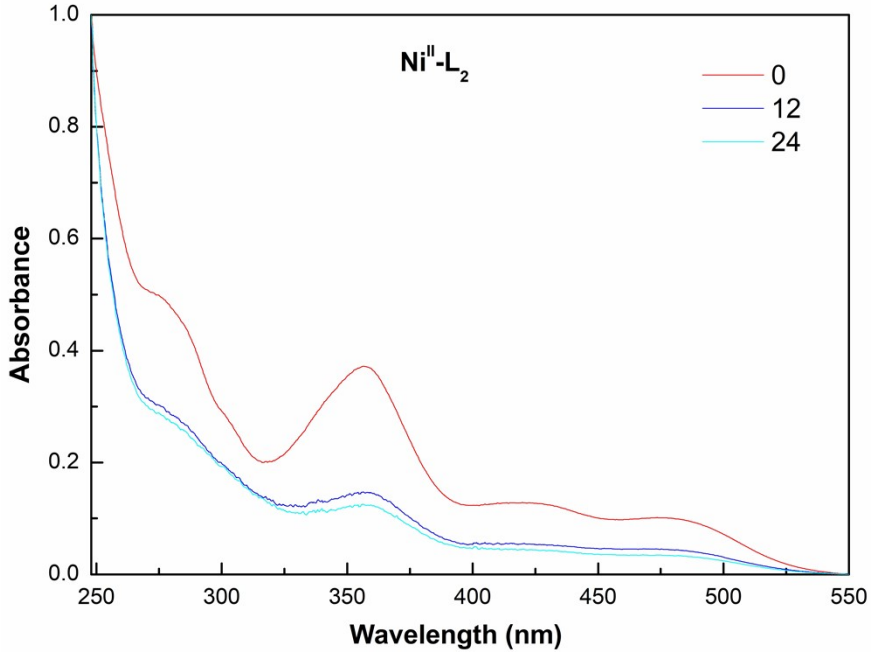

Figure S38. The absorption spectrum of a freshly prepared solution of **Zn^{II}-L_1** in a DMSO:Buffer solution (60:40) and absorption spectral changes after several storage periods. **A)** Contains spectra registered every 3 h, up to 24 h, and in order to ease the visualization, **B)** contains a selection of the spectra obtained for t = 0, 12, and 24 h.

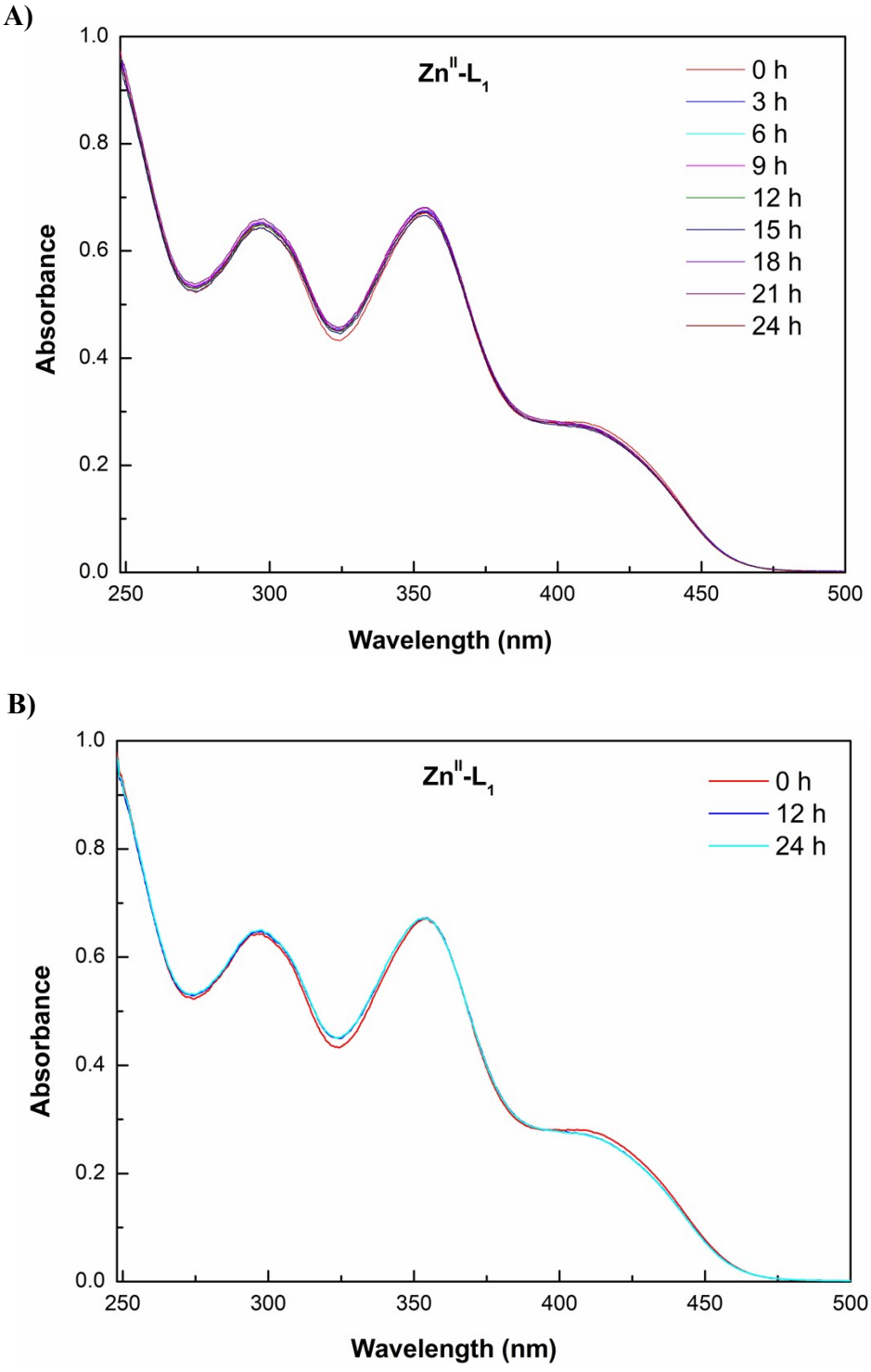

Figure S39. The absorption spectrum of a freshly prepared solution of **Zn^{II}-L_2** in a DMSO:Buffer solution (60:40) and absorption spectral changes after several storage periods. **A)** Contains spectra registered every 3 h, up to 24 h, and in order to ease the visualization, **B)** contains a selection of the spectra obtained for t = 0, 12, and 24 h.

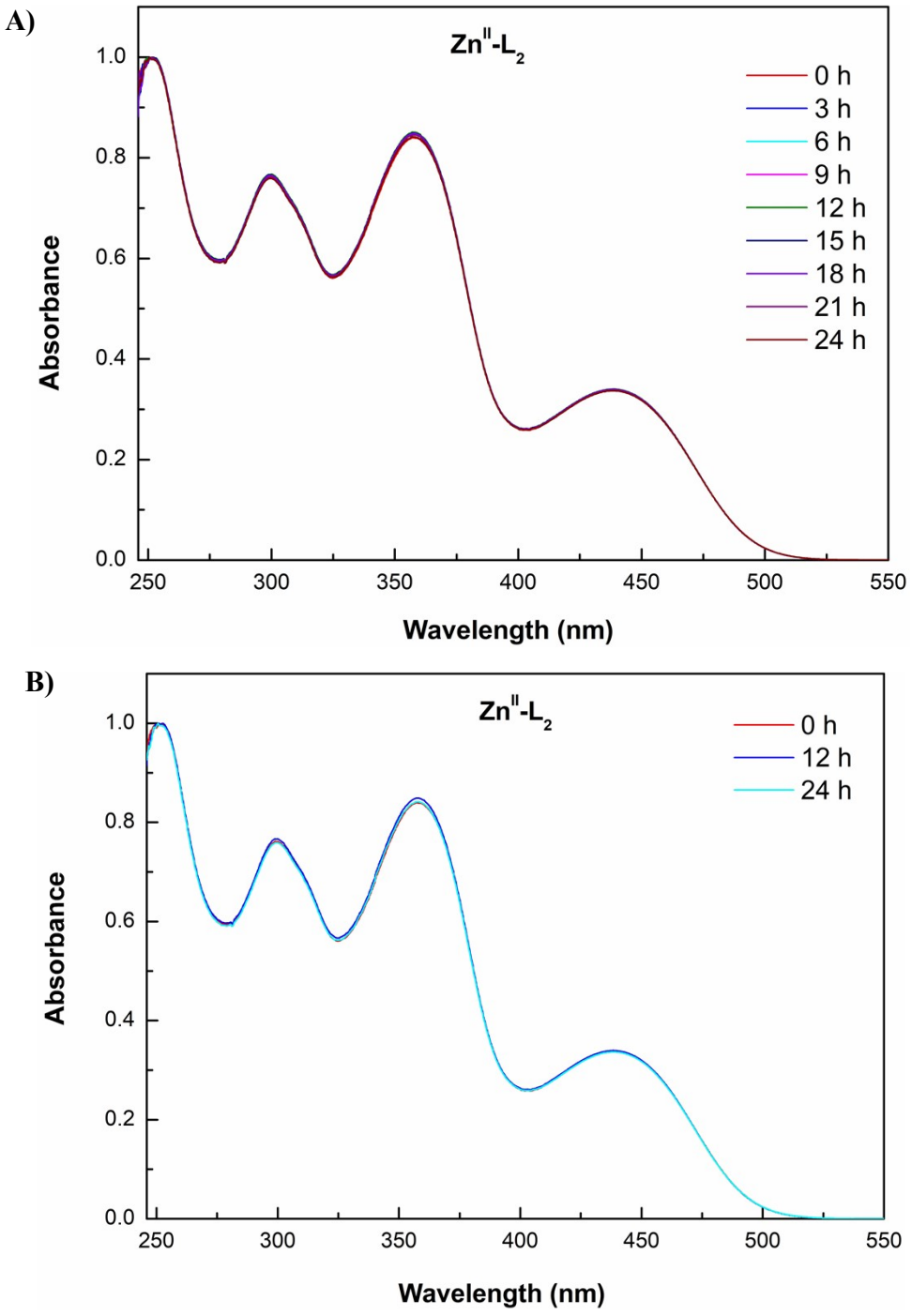

Figure S40. Intermolecular hydrogen bonds C5-H5···O3 and C7-H7···O3 of compound **Ni^{II}-L^1**.

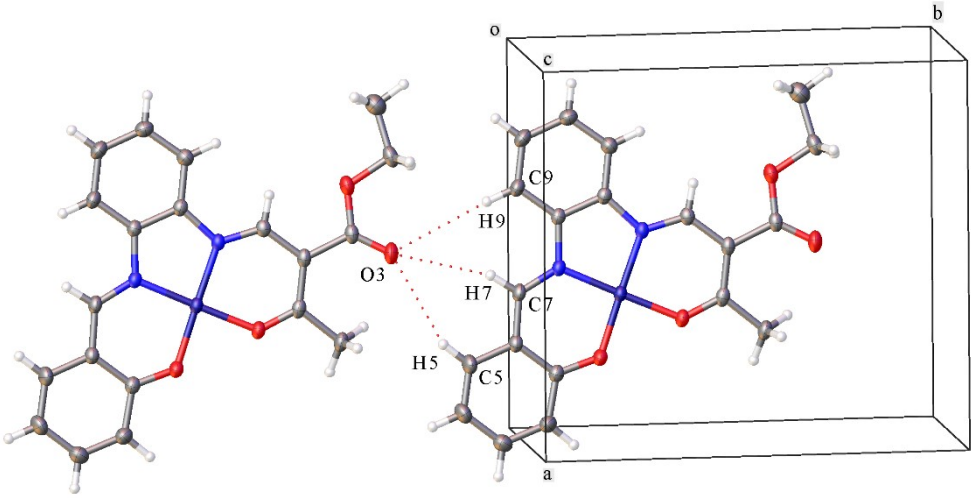

Figure S41. Intermolecular bifurcated hydrogen bond C19-H19A···O1 and C19-H19A···O2 of compound **Ni^{II}-L^1**.

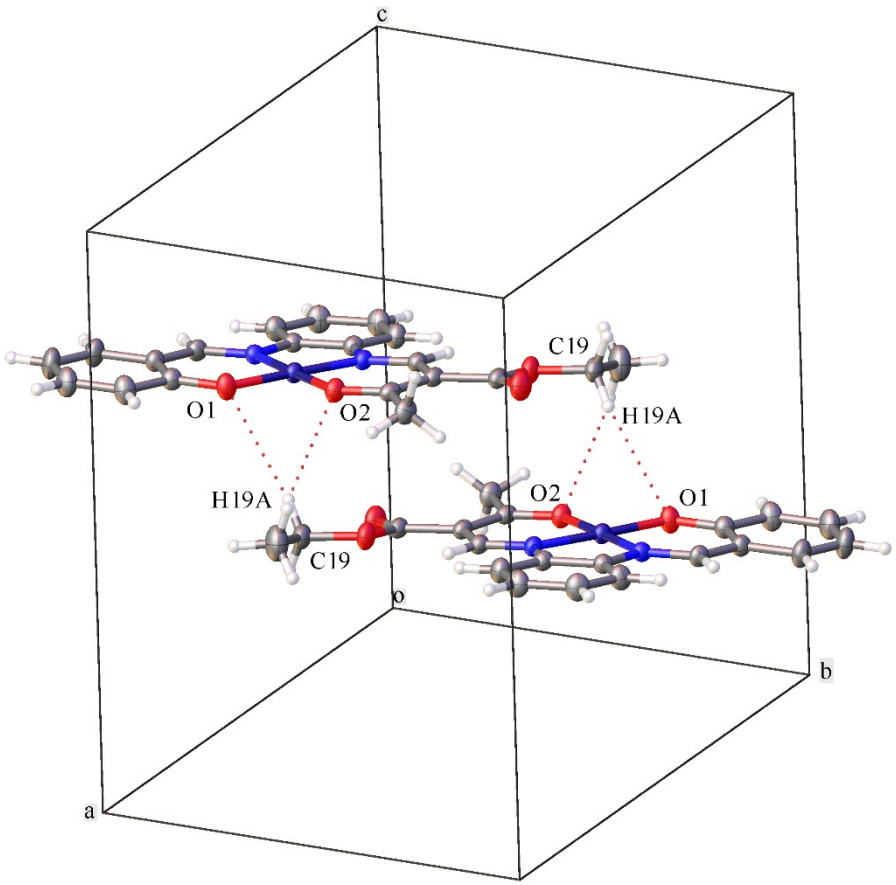

Figure S42. Intermolecular hydrogen bonds C21-H21C···O5 of compound **Ni^{II}-L^2**.

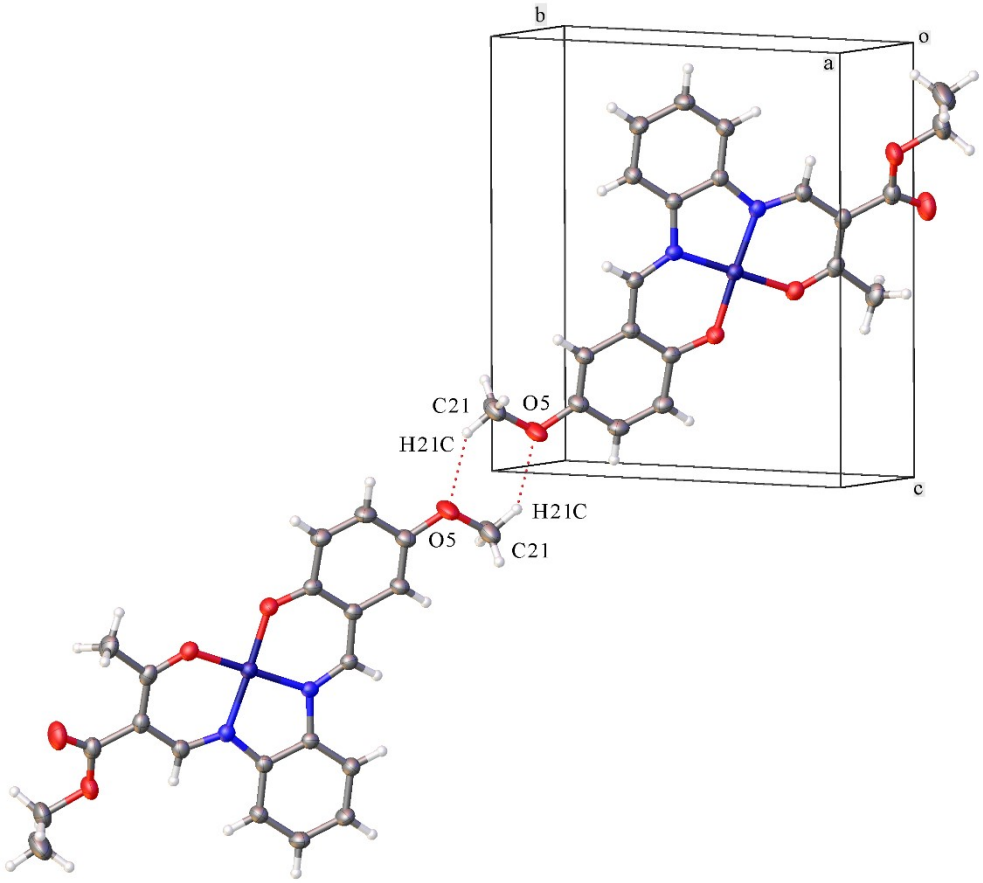

Figure S43. Intermolecular hydrogen bonds C19-H19B···O1 of compound **Ni^{II}-L^2**.

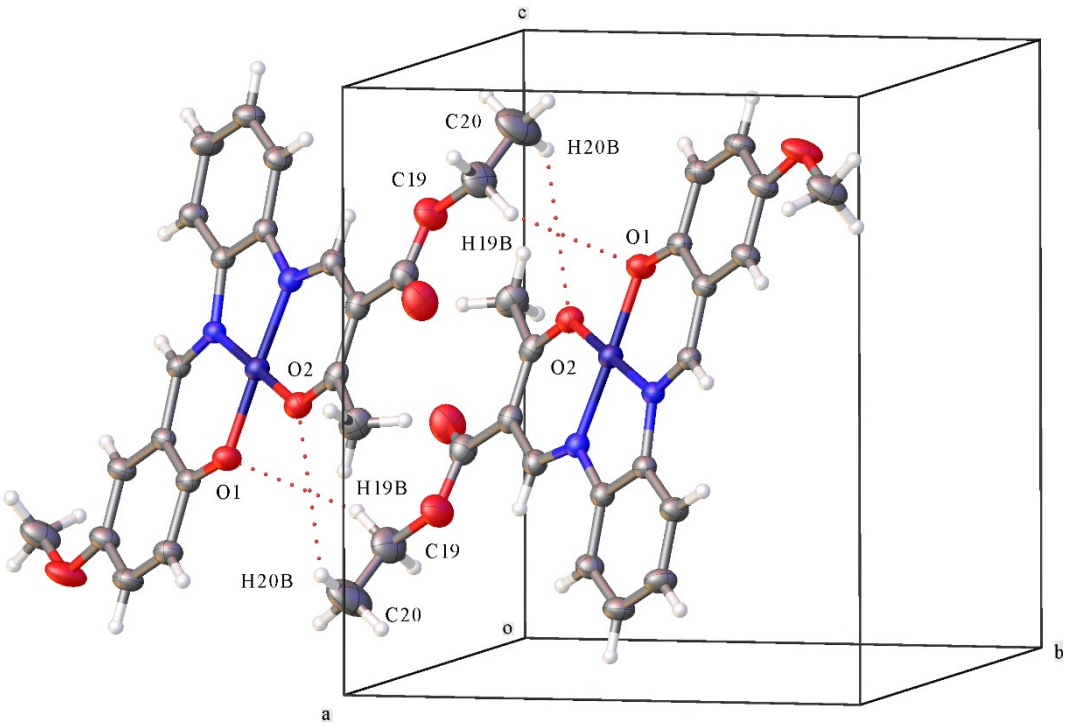

Figure S44. Cell viability assay on MG-63, HCT-116 and MDA-MB-231 cells after 24 of incubation with ligands (**H_2L^1 and H_2L^2**), Ni(II) complexes (**Ni^{II}-L^1 and Ni^{II}-L^2**) and Zn(II) complexes compound (**Zn^{II}-L^1 and Zn^{II}-L^2**). The results are expressed as the percentage of the basal level and represent the mean ± the standard error of the mean (SEM) (n = 18). Asterisk signficant difference in comparison with the basal level ($p < 0.01$).